N-Terminal Beta Amyloid Fragments Regulate Nicotinic Acetylcholine Receptors

A dissertation submitted to the graduate division of the University of Hawai'i at Mānoa in partial fulfillment of the requirements for the degree of

Doctor of Philosophy

in

Cell & Molecular Biology (Neurosciences)

December 2014

By

James Le Marchant Lawrence

Dissertation Committee

Robert Nichols, Chairperson
Marla Berry
Martin Rayner
Alexander Stokes
George Hui

Acknowledgments

I would first like to thank the CMB faculty admissions committee for giving the chance to pursue this course of study to someone such as me, at my age and with such a peculiar educational and career history, you may never know what a profound impact your decision had on my life. Of that number several have then gone on to provide extraordinary levels of inspiration, education and guidance, none more so than Dr. Robert Nichols, a polymath in whom I remain in awe. Thank you for accepting me into your lab, providing such a supportive and exciting environment to work in, actively teaching me so many things on so many different topics and guiding me through this entire project.

I also want to acknowledge the invaluable input from other members of the faculty, starting with Dr Claire Wright and Dr Joshua Astern for teaching me the essential tools of research, Dr Olivier Le Saux for his help with education on the fundamentals of CMB, Dr Alex Stokes for his continuous availability for my interminable questions and his creative suggestions to my research issues, Dr Peter Hoffman for his patient help with both the theory and practical aspects of experimentation, Dr Cedomir Todorovic and Dr Tessi Sherrin not only for their collaboration on this project but also for their help and guidance on many aspects of my work, Dr Marla Berry for always being available on any subject and finally to Dr Martin Rayner for his unyielding support from long before I arrived at JABSOM. Much appreciation must also be given to my colleagues, to Dr Mei Tong for her early work on this project, for Dr Komal Arora, Naghum Alfulaij and Kelly Forest for being such terrific, intelligent and fun people to work with.

Finally I have to thank the people who mean the most to me, and without whom none of this would be possible let alone worthwhile. To my wife Brooke, my kids Momi and Nanea, whose love means

everything, you are truly what I live for. Lastly, to my Mum and Dad who will always be my examples of how to live a good life, thank you for everything.

Abstract

Soluble β-amyloid (Aβ) has been shown to regulate both presynaptic Ca^{2+} and synaptic plasticity. In particular picomolar concentrations of Aβ were found to have an agonist-like action on presynaptic nicotinic receptors and to augment long-term potentiation (LTP) in a manner dependent upon nicotinic receptors. Here we have found that a functional N-terminal domain containing two histidine residues exists within Aβ that accounts for its agonist-like activity. This sequence corresponds to an N-terminal fragment generated by the combined action of α- and β-secretases, and a resident carboxypeptidase. The N-terminal Aβ fragment is present in the brains and CSF of healthy adults as well as Alzheimer's patients. Unlike full-length Aβ, the N-terminal Aβ fragment is monomeric and nontoxic. In Ca^{2+} imaging studies using a model reconstituted rodent neuroblastoma cell line and isolated mouse hippocampal nerve terminals, the N-terminal Aβ fragment proved to be highly potent and more effective than full-length Aβ in its agonist-like action on nicotinic receptors. In addition, the N-terminal Aβ fragment augmented theta burst-induced post-tetanic potentiation and LTP in mouse hippocampal slices. The N-terminal Aβ fragment also rescued LTP inhibited by elevated levels of full-length Aβ. Contextual fear conditioning was also strongly augmented following bilateral injection of N-terminal Aβ fragment into the dorsal hippocampi of intact mice. The fragment-induced augmentation of fear conditioning was attenuated by coadministration of nicotinic antagonist. The activity of the N-terminal Aβ fragment appears to reside in a sequence surrounding a putative metal binding site at its the C-terminal region, YEVHHQ. This sequence is sufficient to both produce the aforementioned agonist-like action on nicotinic receptors in our rodent neuroblastoma cell line and augment fear conditioning in our mouse model. In addition to either the basic or aromatic properties, of the two histidine residues in the sequence it also appears that the aromatic properties of the initial tyrosine are required for the activity.

These finding suggest that the N-terminal Aβ fragment may serve as a potent and effective endogenous neuromodulator.

Table of Contents

List of Figures

Abbreviations

5-HT	= 5-Hydroxytryptamine (serotonin)
Aβ	= Beta Amyloid
αBgTx	= α-Bungarotoxin
ACh	= Acetylcholine
AChBP	= Acetylcholine Binding Protein
AD	= Alzheimer's Disease
ADAM	= A Disintegrin And Metalloprotease
AICD	= APP Intracellular Cytoplasmic/C-terminal Domain
AMPA	= α-Amino-3-hydroxy-5-Methyl-4-isoxazolePropionic Acid
APOE	= Apolipoprotein E
APH-1	= Anterior Pharynx-defective 1
APP	= Amyloid Precursor Protein
BACE1	= β-site APP Cleaving Enzyme 1
BSA	= Bovine Serum Albumin
CA1	= Cornu Ammonis 1
cAMP	= Cyclic Adenosine Monophosphate
CD	= Circular Dichroism
CSF	= Cerebral Spinal Fluid
DMEM	= Dulbecco's Modified Eagle's Medium
EDTA	= Ethylenediaminetetraacetic acid
ER	= Endoplasmic Reticulum

FBS	= Fetal Bovine Serum
fEPSP	= Field Excitatory Postsynaptic Potentials
pEPSP	= Population Excitatory Postsynaptic Potentials
GABA	= γ-Aminobutyric Acid
GPI	= Glycosylphosphatidylinositol
HAT	= Hypoxanthine Aminopterin & Thymidine
HBS	= HEPES-Buffered Saline
HBST	= HBS containing 100nM TTX
IP_3	= Inositol Triphosphate
LTP	= Long-term Potentiation
MALDI-TOF	= Matrix-Assisted Laser Desorption/Ionization Time of Flight
MALS	= Multi Angle Light Scattering
MCI	= Mild Cognitive Impairment
mGluR	= Metabotropic Glutamate Receptors
MLA	= Methyllycaconitine
nAChR	= Nicotinic Acetylcholine Receptors
NMDAR	= N-Methyl-D-Aspartate Receptors
paGFP	= Photoactivatable Green Fluorescent Protein
PALM	= Photoactivated Localization Microscopy
pamCherry	= Photoactivatable Monomeric Cherry Flurorescent Protein
PBS	= Phosphate Buffered Saline
PEN-2	= Presenilin Enhancer 2
PKA	= Protein Kinase A
PKC	= Protein Kinase C

PrP^{c}	= Cellular Prion Protein
PrP^{Sc}	= Scrapie Prion Protein
PTP	= Post Tetanic Potentiation
SDS-PAGE	= Sodium Dodecyl Sulfate – Polyacrylamide Gel Electrophoresis
SELDI-TOF	= Surface-Enhanced Laser Desorption/Ionization Time of Flight
SEM	= Standard Error of the Mean
STI1	= Stress-Induced Protein 1
TBP	= Theta Burst Protocol
ThT	= Thioflavin-T
TM	= Transmembrane domain
TTX	= Tetrodotoxin
WT	= Wild-Type

Chapter 1

Introduction

1. Background

1.1 *Alzheimer's Disease*

Alzheimer's Disease (AD) is a neurodegenerative disorder that is the most common type of dementia and was the 6th most common cause of death in the United States in 2012, affecting 1 in 8 Americans over the age of 65 and costing an estimated $200 billion[1]. It was first reported in 1906 by Alois Alzheimer, who described the progress of clinical symptoms of a 51-year-old woman through to her death at age 55. Post-mortem examination of the patient's brain showed widespread neocortical atrophy as well as the presence of amyloid plaques (insoluble fibrous protein aggregates) and neurofibrillary tangles[2].

The diagnostic criteria have recently been revised to include 3 stages of the disease[3] beginning with a preclinical phase, where only biomarkers are detectable but no other symptoms. The observable clinical manifestations may begin with mild cognitive impairment (MCI), often described as a prodromal phase, wherein the patient and/or close relatives or friends note impairment in recent memory formation and recall, with unaffected remote memory function[4]. Most, but not all, patients with MCI progress to the third and final stage, now known as dementia due to Alzheimer's disease, where patients experience a wide variety of additional symptoms usually starting with challenges to executive function such as problem solving or attention, and spreading into language dysfunction, time and space confusion, visuospatial difficulty, loss of insight and personality changes and ending with loss of long-term memory, ability to perform activities of daily living, bowel and bladder control and finally culminating in death[5,6].

Unsurprisingly, the progressive neurodegeneration involved plots a sequential path through the areas of the brain, and neuronal subpopulations, related to the altered functions. Hence, the disorder starts with the neurons of the entorhinal cortex, particularly those in layer II, which process both the inputs and outputs of the hippocampus, as well as the pyramidal neurons of the hippocampus, especially those in the CA1 area[7]. These areas, found in the medial temporal lobe, are vital for the formation of new memories. The pathology then spreads to the frontal (executive functioning), cingulate (emotion formation and processing) and parietal (visuospatial integration) cortices. The most vulnerable subpopulation of neurons are glutamatergic; however, the cholinergic neurons in the basal forebrain, the adrenergic neurons in the locus coeruleus and the serotonergic neurons of the raphe nuclei are also affected to varying degrees, further accounting for the effects on attention, spatial memory, arousal, vigilance, aggression and mood[6,8]. The basal forebrain cholinergic neurons, which project widely across the brain, actually undergo significant degeneration, leading to a general cholinergic deficit. However, the functional deficits are not confined to the loss of any particular neurotransmitter, such as the loss of dopamine in Parkinson's disease, but are primarily due to degradation of neural networks. Intriguingly one of the first such networks to be affected is the "default mode network", which has the highest baseline neuronal activity in the resting state[9] and encompasses several posterior cortical regions including the posterior cingulate cortex[10]. Alterations in the default network have been shown to affect AD pathology[11,12].

The underlying molecular mechanisms involved in this neurodegeneration, which begins with synaptic failure and ends with neuronal death, were first alluded to in Alzheimer's postmortem examination, with the noted amyloid plaques eventually being identified as consisting of isoforms of the protein beta amyloid (Aβ) and the neurofibrillary tangles being hyperphosphorylated Tau protein, a microtubule-associated protein. However, the interactions between these two proteins and the mechanisms by

which they lead to synaptic dysfunction are still under investigation, although it is known to include an inflammatory response, axonal transport dysfunction and oxidative stress[6]. What is abundantly clear is that levels of Aβ and Tau begin to rise in the preclinical stage and the former can be detected anywhere from 10 to 20 years before the onset of symptoms[13].

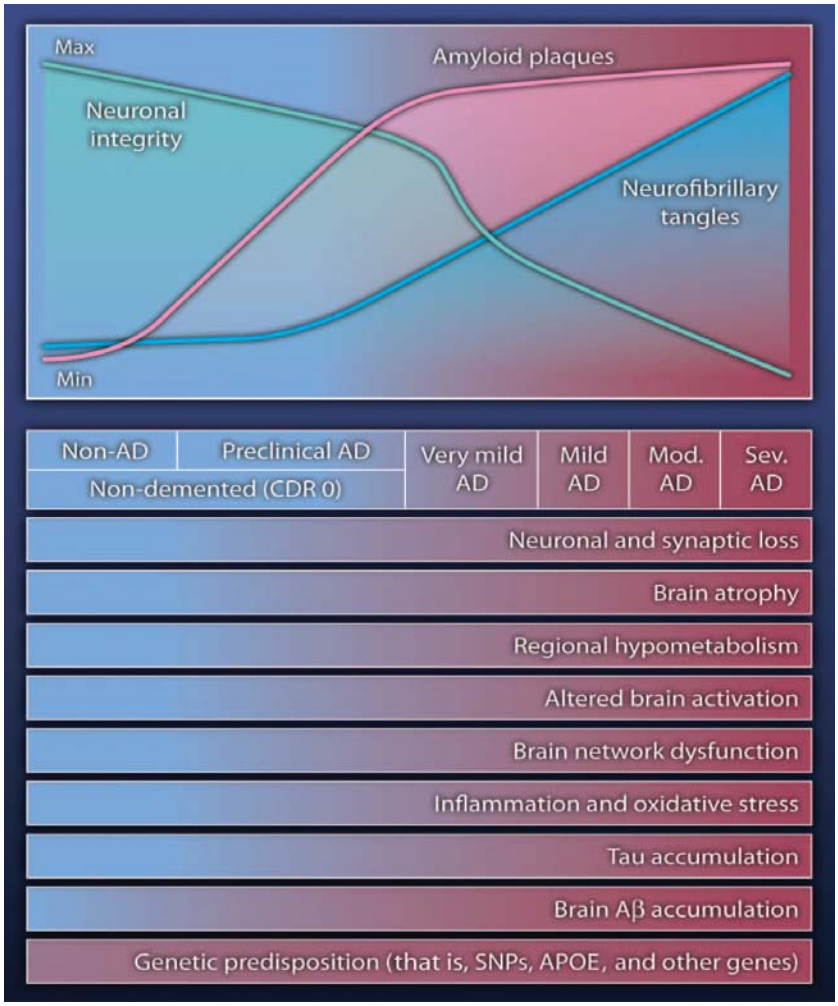

Figure 1. Graph showing interrelation between various aspects of AD pathology and clinical presentations (taken from6).

Note that the rating of AD is using the old system; current terminology equates very mild AD as MCI and mild, moderate and severe AD as dementia due to Alzheimer's disease[1].

Although this chart sets out the rise in amyloid plaques (consisting of aggregates of β sheets as opposed to non-fibrillar diffuse plaques), which are the pathological hallmarks of the disease, their location is strongly correlated with cellular inflammation but not with the antecedent synaptic loss[13]. This event is, however, highly correlated with high levels of soluble low-n Aβ oligomers[14], which are the precursors to fibril formation.

Increasing concentrations of soluble Aβ in late-onset AD, the most common form, were found to be a result, not of overproduction, but of a dysfunction in the mechanisms involved in its clearance[15]. Indeed the greatest risk factor for late-onset AD is the presence of the ε4 allele of Apolipoprotein E (APOE), as opposed to the ε2 allele, which is more neuroprotective[16]. The strongest evidence to date suggests that APOE normally acts not only as a scaffold protein involved in the proteolytic degradation of soluble isoforms of Aβ[17] but also interferes with the seeding and polymerization of Aβ[18], thus preventing the formation of fibrillar aggregates, and that the ε4 allele does this poorly, whereas this activity is enhanced by the ε2 allele[6].

The fact that Aβ is produced during normal cellular metabolism *in vivo* as well as *in vitro*[19] and is found in the 200pM range in normal human[20] and mouse brain[21] implies that it may have some physiological function. Finding any physiological function(s), therefore, is essential, particularly because clearing Aβ before amyloid plaques form presents itself as a highly attractive option for preventing AD.

1.2 *Amyloid Precursor Protein (APP) & Aβ Production*

Aβ is comprised of several isoforms that are produced by the sequential enzymatic cleavage of APP, the latter a Type I (single pass) transmembrane protein with an intracellular C-terminal and extracellular N-terminal. APP is expressed in many tissues but is preferentially targeted to synaptic membranes[22]. The human gene for APP is located on chromosome 21 and contains at least 18 exons. Unsurprisingly, it has several isoforms, the most common of which are 695, 751 and 770 amino acids in length[6], with the former being the dominant form in neurons and neuron-specific[23], however; references to the numbering of amino acids in this dissertation are made to the 770 amino acid isoform. The trisomy of this chromosome in Down's syndrome individuals leads to the overproduction of APP and explains why

all such individuals develop an early onset form of AD, and in fact, led to the discovery of the gene's location[6]. Indeed, in the rare cases where the APP allele is not copied in a Down's patient, no amyloid plaques were found to be present[14].

The first 17 amino acids of APP act as the signal peptide, whilst the transmembrane region consists of the amino acids located in positions 700-723. After post-translational modification in the endoplasmic reticulum (ER) and Golgi apparatus, mainly phosphorylation, glycosylation and tyrosine sulfation[24], proteolytic processing of APP occurs primarily through the action of 3 families of secretases as shown in (Fig. 2).

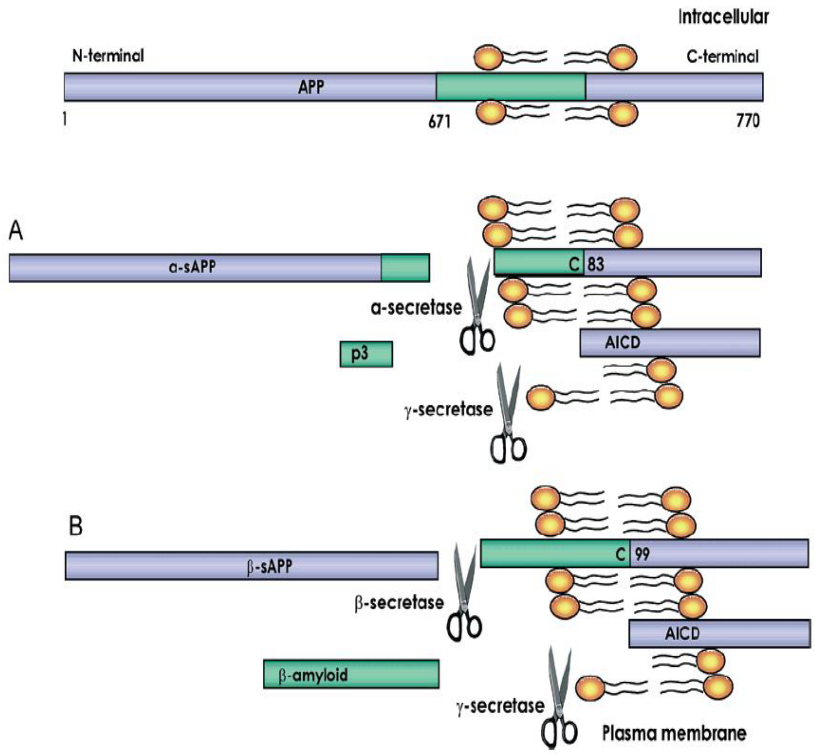

Figure 2. Classical proteolytic cleavage pathways of APP[25]

(A) Non-amyloidogenic pathway – cleavage by α then γ secretases produces sAPPα, the p3 fragment and an APP Intracellular C-terminal Domain (AICD)

(B) Amyloidogenic pathway – cleavage by β then γ secretases produces sAPPβ, Aβ and an AICD

Cleavage of APP by α-secretases is the essential step in the non-amyloidogenic pathway, as they cleave APP within the sequence that would produce Aβ. They consist of members of the ADAM family of zinc metalloprotease integral membrane glycoproteins[26,27], which cleave APP between the lysine at position 687 and the leucine at position 688 and do so in both an unregulated manner at the cell surface[28] and a protein kinase C (PKC)-dependent manner in the trans-Golgi network[29]. The PKC regulated processing of APP by α-secretase was found to be competitive with processing of APP by β-secretase[29]. The discovery of this competition led to the idea of mutual exclusivity of the two pathways shown in Figure. 2.

β-secretase was found to be a Type I transmembrane aspartyl protease of the pepsin family, named β-site APP Cleaving Enzyme 1 (BACE1), that cleaves APP between the methionine at position 671 and the aspartate at 672 via its extracellular cleavage domain[30]. BACE1 displays optimal activity at pH 4.5[31] and the upregulation of α-secretase by PKC activation reduces the amount of BACE1 cleavage[29], although APP localized to lipid raft microdomains is preferentially cleaved by BACE1 compared to α-secretase[32].

Genetic mutations of APP involved in the familial versions of early onset AD include one found in a Swedish-family whereby the lysine in position 670 is substituted by an asparagine and the methionine at position 671 is substituted by a leucine[33]. These mutations increase the affinity of the peptide to BACE1 and hence upregulate BACE1 cleavage of APP and the resultant production of Aβ isoforms, therefore this mutated sequence has been a useful tool in both *in vitro* and *in vivo* studies.

The final secretase, γ-secretase, is yet to be fully characterized but is known to be an integral membrane multimeric protein complex composed of at least four components: presenilin, nicastrin, anterior pharynx-defective 1 (APH-1) and presenilin enhancer 2 (PEN-2)[34], with presenilin containing the

transmembrane aspartyl protease domain[35]. There is also evidence that the γ-secretase complex is associated with lipid raft microdomains in the ER, trans-Golgi network and endosomes[34]. Once APP has been cleaved by α or β-secretases, the remaining membrane-bound fragment (C83 or C99) is cleaved in its transmembrane sequence by γ-secretase at a variety of positions (Fig. 3).

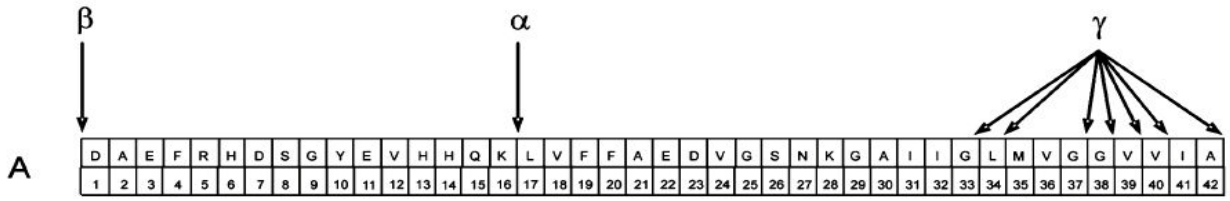

Figure 3. Known cleavage sites for α, β and γ-secretase in Aβ amino acid sequence[25].

The presence of the multiple cleavage sites of γ-secretase means that the sequential cleavage of APP by β- then γ-secretases can create several different possible isoforms of Aβ, namely 1-42, 1-40, 1-39, 1-38, 1-37, 1-34 and 1-33, whilst non-classical sequential cleavage of APP by β- then α-secretases would be required to produce an Aβ fragment from 1-16. The actual abundance of Aβ isoforms found to be present in human non-AD CSF is shown in Figure. 4.

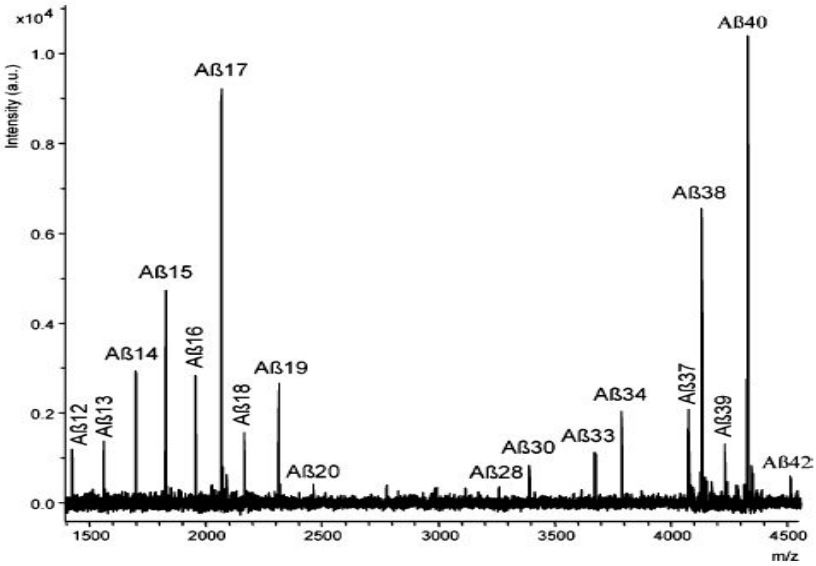

Figure 4. Abundance of Aβ isoforms in human CSF detected by immunoprecipitation and subsequent MALDI-TOF[25]

These results were initially both expected and surprising, as it was well established that the ratio of $A\beta_{1\text{-}40}$, the non-amyloidogenic

and most abundant isoform, to $A\beta_{1-42}$, the most amyloidogenic isoform, was 10:1 and that γ-secretase cleavage of the former occurs in the ER whereas it occurs in the trans-Golgi network for the later[36]. It was also known that mutations to presenilin genes (PSEN1 & PSEN2), which have been shown to be present in both early and late onset AD, increased the ratio of production of the 1-42 isoform as compared to the 1-40 isoform[6]. However, what was surprising was the relative abundance of smaller fragments whose cleavage sites, apart from the 1-16 isoform, do not tally with those of the known secretases, nor did the classical cleavage pathways account for the presence of 1-16.

Manipulation of an *in vitro* model with γ-secretase inhibitors decreased the presence of all isoforms longer than 1-16 in the extracellular fluid, which would imply that the 1-17 isoform, notable by its abundance in CSF, requires γ-secretase activity[37]. If this cleavage between the leucine at position 17 and the valine at position 18 were to be carried out by γ-secretase itself, the C99 fragment produced by prior β-secretase cleavage would have to change conformation such that this new cleavage site became accessible to γ-secretase, which normally cleaves within the membrane. Another possibility is that γ-secretase activity affects another, as yet unknown, protease, or that such a protease is affected directly by γ-secretase inhibitors. A non-exhaustive list of potential candidate enzymes for various cleavage sites that would explain the fragments found in CSF is shown in Figure. 5.

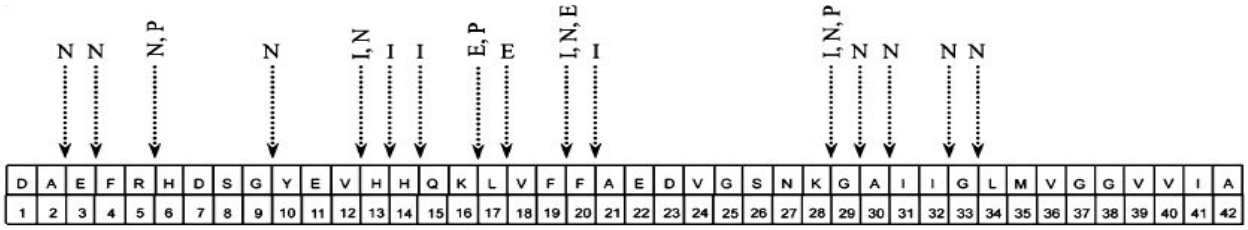

Figure 5. Amino acid sequence for $A\beta_{1-42}$ with known enzyme cleavage sites relating to N-terminal fragments

N = neprilysin; P = plasmin; I = insulin-degrading enzyme ; E = endothelin-converting enzyme (ECE-1, ECE-2)[25]

The same authors also found that all the shorter N-terminal Aβ fragments (less than 1-17) were dependent on both α- & β-secretase activity[37], and thus the relative abundance of these shorter fragments points to the physiological frequency of the non-classical pathway. It should also be noted that these authors discovered a conversion of the 1-16 fragment into 1-15 through the activity of carboxypeptidase(s) in the fetal bovine solution used as a buffer in their assay[38], and others have found both carboxypeptidase types B and E, which are capable of cleaving the lysine at position 16, to be present in hippocampi[39,40].

A final important aspect of Aβ production is that it has been found to be dependent upon action potential-generated synaptic activity and that activity requires both exo- and endocytosis, with increased activity increasing production and decreased activity suppressing it[41,42].

1.3 Aβ synaptic effects

Pathological levels (nM-μM) of Aβ oligomers have been shown to significantly decrease glutamatergic synaptic transmission and induce a subsequent loss in dendritic spines, involving a reduction in post-synaptic AMPA- and NMDA-type glutamate receptors[43,44]. However, in view of the tight synaptic regulation of Aβ production under physiological conditions, it appears that a slight, transient depression of synaptic activity due to a small, transient increase in Aβ production to nM might be part of a neuromodulatory mechanism referred to as synaptic scaling[45]. Clear evidence for the role of Aβ as a neuromodulator was discovered for Aβ at low picomolar levels, where it was found to increase hippocampal long-term potentiation (LTP) *ex vivo* and also enhance both reference memory and contextual fear memory[21]. Furthermore, the same group found that these enhancements involved α7-type nicotinic acetylcholine receptors, that endogenous Aβ is necessary for hippocampal synaptic plasticity, and its related memory mechanisms, and that this effect is due to alterations in presynaptic

vesicle release frequency[46]. This positive modulation of synaptic activity is further supported by evidence showing synaptic transmission decreases in mice with abnormally low levels of Aβ[47].

The involvement of nAChR is unsurprising given their widespread pre-, peri- and post-synaptic location and the fact that there is substantial loss and dysfunction in basal forebrain cholinergic neurons in the progression of AD[6]. For the sake of clarity, however, nAChR are not the only receptors that interact with Aβ, as some form of interaction has been found with NMDA receptors (NMDAR)[47] and several G-protein coupled receptors including both metabotropic glutamate receptors (mGluR)[48] and amylin receptors[49].

1.4 *Nicotinic Acetylcholine Receptors (nAChR)*

The nAChR are non-selective cationic channels that are members of the "Cys-loop" class of the superfamily of ionotropic (ligand-gated ion channel) receptors that includes $GABA_A$, $GABA_C$, glycine & 5-HT_3 receptors[50]. All of these receptors form homologous pentamers, conserved across many species.

The nAChR can be broadly categorized as muscle or neuronal type with the former being comprised of two α_1 subunits and one each of β_1, δ and either γ or ε subunits, whilst the latter, which are the focus of this dissertation, are either homomers of α-subunits (e.g. α7) or heteromers that have to include at least two α-subunits (e.g. α4) along with β-subunits (e.g. β2)[50].

Each subunit, as shown in Figure 6, consists of three key structural regions; a large extracellular N-terminal domain, four transmembrane domains (TM1-4), and a large cytoplasmic loop between TM3 and TM4. They also contain 2 shorter loops, one cytoplasmic and one extracellular, as well as an extracellular C-terminal domain [51].

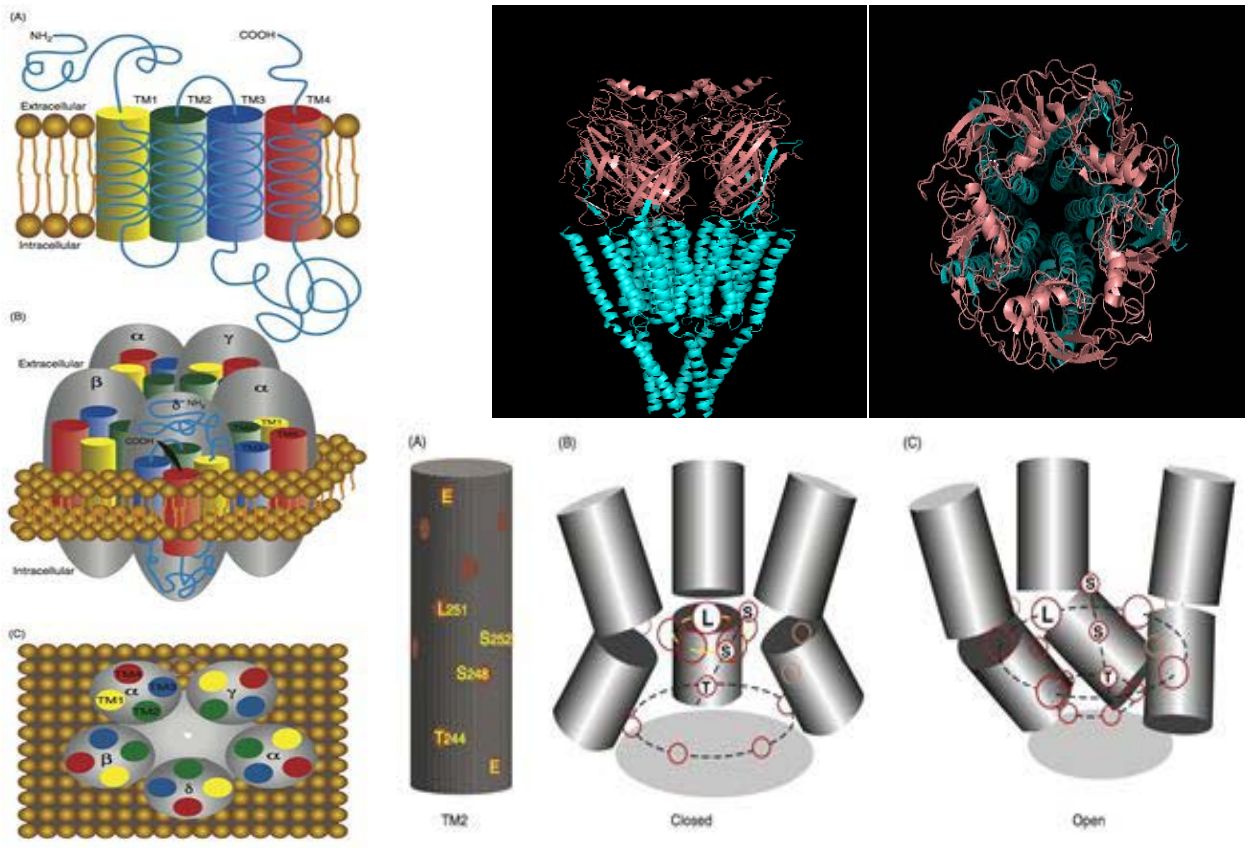

Figure 6. nAChR structure

Arrangement of transmembrane domains in embryonic muscle type nAChR pentamer subunits (left)[52]; rendering of ribbon maps for *Torpedo* nAChR from electron microscope data taken at 4 angstroms[53] (top right); model of 3 of α_1 TM2 regions showing conformational changes, and effect on leucine ring pore, between closed and open states of nAChR[52]

The primary agonist binding sites for acetylcholine (ACh), nicotine and the competitive antagonist α-bungarotoxin (αBgTx), are located in a pocket created by the N-terminal domains of two adjacent subunits, with an α-subunit providing 3 sequence loops (A, B & C) that act as the principal binding site and its neighbor, whether α or β, providing 3 sequence loops (D, E & F) that act as a complementary site[54]. The binding pocket is located roughly 40Å from the surface of the plasma membrane[53]. The

residues that are conserved across species, from the receptor of the electric organ of the *Torpedo marmorata*[53] to the acetylcholine binding protein (AChBP) of the snail *Lymnaea stagnalis* (an analog of the extracellular domain of the α7 receptor)[55], are all aromatic, with four being tryptophan and three being tyrosine[54]. We discovered that one of these residues, the tyrosine located in loop C of the N-terminal domain at position 188 in mouse α7 homomeric nAChR (α7-nAChR), was critical for the activation of the receptor by $A\beta_{1-42}$[56]. In addition to this binding pocket multiple allosteric binding sites have also been located, many found in the transmembrane domains, which have a variety of modulatory effects on the receptors' function[54].

As shown in Figure 6, the ion pore is created by the arrangement of the four transmembrane domains, with TM2 facing inward and thus being primarily responsible for both ion selectivity and allowing passage of ions through the channel[51]. However there is some evidence that a ring of negatively charged residues in the extracellular domain that are arranged around the mouth of the pore may contribute to cation selectivity[57]. Figure 6 also highlights the conformational change in the TM2 domains that leads to the channel gate opening, with a rotation about the TM2's axis causing the hydrophobic leucine ring in the heart of the pore to expand its radius from 6Å to 9Å, thus allowing the passage of K^+, Na^+ and Ca^{2+} [53]. In addition, the conformational change leads to a string of neutrally hydrophobic/hydrophilic residues lining up to assist with the passage of these ions through the pore[51].

The large cytoplasmic loop located between TM3 and TM4 has been shown to be involved in assembly of the receptors, their targeting and trafficking to the membrane[58], as well as containing signaling sequences and sites for receptor phosphorylation by both PKA and PKC[59].

The receptors exist in four distinct states: channel closed with no ligand bound (resting), channel open with ligand bound (open), a desensitized state where the channel is closed with ligand bound with high affinity (desensitized) and an inactivated state, which is a long-lasting desensitized state[60]. Each receptor composition of the differing subunits has an effect on the speed of transition and duration of each of these states[61], as well as the relative permeability to different cations, particularly Ca^{2+} [62]. Whether the transitions between states are linear following ligand binding or are spontaneous and ligand binding merely stabilizes each conformation is unclear. However, what is known is that the conformational change to the open state is a global one involving, in particular, reorganizations of both the extracellular domain and the transmembrane domains. Such changes occur rapidly (in the order of µs to ms) and occur at a relatively low binding affinity of the ligand[54]. Following the open state, the receptors transition into the desensitized state, in a receptor subunit- and ligand concentration-dependent manner, with the α7-containing nAChR desensitizing in ms[61]. The precise conformational changes involved are as yet unclear; however, it is likely to involve a tightening of the binding pocket, as evidenced by the increased ligand binding affinity (~100 fold & in the order of µM) and an additional change within TM2 explaining the lack of ion movement[63]. The structures responsible for the differences between subunit desensitization rates have been isolated to the interface between the extracellular and transmembrane domains[64]. The recovery from desensitization is also subunit-dependent, with the homomeric α7-nAChR taking about a second to be available for reactivation[64], and possibly modulated by the phosphorylation of the large cytoplasmic loop[63].

The distribution of nAChR throughout the body is widespread, having been found throughout the nervous system, muscles, as well as other non-neuronal tissue, where they are involved in cell-to-cell signaling (e.g. in leukocytes[50]). Expression of nAChR within the brain is also found in many diverse areas including the cortex, striatum, cerebellum, brain stem, diencephalon and hippocampus[54]. The subtype

with the highest and most diffuse levels of expression is the α4β2[50]receptor. In contrast, the homomeric α7 subtype (α7-nAChR) is not only highly expressed in the hippocampus, the structure essential for formation of new memories, but has been found to be present in nearly all synapses in its crucial CA1 region[65], making α7-nAChR of great interest for study in AD. Indeed, although the massive loss of nAChR in the cerebral cortex in AD is predominantly of α4β2 receptors, within the hippocampus the loss is chiefly of α7-nAChR and such loss directly correlates with the progressive loss of cognitive function[54]. Furthermore, Aβ has been found to bind to α7-nAChR with pM affinity[66], and we and others have found that pM concentrations are sufficient to activate them, with maximal activation being at 100nM[67].

Other key aspects of α7-nAChR are their high level of Ca^{2+} permeability, as compared to other subtypes[62], and their predominantly presynaptic location[65]. This suggests an essential role in the release of other neurotransmitters, particularly glutamate and GABA. When this presynaptic function of α7-nAChR is coupled with the data showing coupling of Aβ production with presynaptic activity, the activation of α7-nAChR by low concentrations of Aβ and their inhibition by higher concentrations of Aβ, a picture emerges of a potential neuromodulatory role for Aβ's interaction with α7-nAChR.

2. Hypotheses

2.1 *Overall goal*

To examine the impact of the N-terminal beta amyloid fragments on α7-nAChRs and elucidate the structural-functional determinants for the N-terminal beta amyloid fragments.

2.2 *Central Hypothesis*

The N-terminal Aβ fragments are highly potent activators of presynaptic α7-nAChRs.

We also hypothesize that the critical amino acids in the N-terminal Aβ fragments include a positively charged component that interacts with the π-bonds of the aromatic residues within the binding pocket of the receptor.

2.3 *Rationale*

Soluble Aβ, although toxic at the levels found in AD patients, exists in lower concentrations (pM) in healthy adults apparently without harmful effects[68]. The discovery of a predominantly presynaptic locale for the production of Aβ that is correlated with synaptic activity, combined with the finding of a positive effect of picomolar concentrations of Aβ on LTP and α7-nAChR-dependent fear memory, indicate a physiologically significant neuromodulatory role for Aβ. By contrast, the functional implication of the significant quantities of N-terminal Aβ fragments in healthy adults, the production of which can all be regulated by α-secretase activity, over and above the regulation via axonal activity, has not been examined.

Studies of the interactions between ACh or nicotine and nAChR have shown that the key residues in the binding pocket are all aromatic, being either tyrosines or tryptophans, leading to the assumption that cation-π interactions are involved. This assumption was strengthened by x-ray crystallography data taken at 1.94 Å of an αBgTx molecule bound to the mouse α1 subunit, which showed the close spatial relationship between the guanidinium group of an arginine residue of αBgTx to the homolog of the aforementioned tyrosine[69], and is also reflected in the position of a quaternary ammonium of the nAChR agonist carbamylcholine to the homolog of the same tyrosine in AChBP[70]. It is thus likely that the interaction of Aβ with nAChR would be via a similar mechanism, especially because one of the aforementioned tyrosines has been shown to be essential for α7-nAChR activation by Aβ.

3. Specific Aims

To test my central hypotheses, I formulated the following specific aims

3.1 *SPECIFIC AIM 1*

To examine the functional activity of the N-terminal Aβ fragments and their structural determinants on presynaptic α7-nAChRs

Specific Rationale

We have found a tyrosine in the binding pocket of α7-nAChR, Y188, was essential for the activation of the receptor by both $A\beta_{1-42}$ and ACh, but not nicotine[56]. It is believed that the interaction of the ACh with the aromatic residues in the binding pocket involves cation-π interactions. $A\beta_{1-42}$ consists of a hydrophobic transmembrane domain from residues 29-42 and a hydrophilic extracellular domain consisting of the first 28 residues. It is therefore likely that the essential residues involved in Aβ binding are located in the hydrophilic domain.

$A\beta_{1-42}$ (4514 Da) has been shown to form SDS-stable small oligomers, structural analyses of which have indicated the presence of a random coil structure in the first 14 residues, β-sheets from 15-21, 24-32, 35-37, 40-42 and a turn involving the glutamate at 22 and the aspartate at 23[71]. Even in the conformation that leads to the formation of toxic oligomers, where an additional turn involving the glycine at 38 and the valine at 39 is induced, the random coil structure of the first 14 residues remains exposed[72], as shown by solid-state nuclear magnetic resonance imaging.

The oligomeric status of the N-terminal Aβ fragments is currently unknown. Should they form oligomers, it is possible that the exposure of the active residues may be prevented and thus they would fail to functionally interact with the binding pocket of the nAChR.

The data on αBgTx binding to the α1 subunit of nAChR indicate that this interaction involves finger I of the toxin[69]. We postulated that the N-terminal Aβ fragments may possess a similar finger structure to αBgTx, and that the oligomeric state may have a direct effect on the fragments' functional effects.

3.2 *SPECIFIC AIM 2*

To examine the minimum amino acid sequence responsible for the functional activity of the N-terminal Aβ fragment and to identify the essential components of such sequence

Specific Rationale

Our work pursuant to specific aim 1 led us to the discovery that the active component of the N-terminal Aβ fragment $A\beta_{1\text{-}15}$ lay in its C-terminal region. Accordingly the elucidation of the key molecular components of this sequence, and their interactions could lead to the development of a neuromodulatory peptidomimetic.

4. Experimental Design

The primary approach to examine the effects of N-terminal Aβ fragments on presynaptic α7-nAChR was to use the well established and defined *in vitro* presynaptic model: the NG108-15 rodent hybrid neuroblastoma cell line. Upon differentiation via application of 1mM dibutyryl-cyclic adenosine monophosphate (db-cAMP) in culture media, containing reduced serum (1%), these cells elaborate neurites containing presynaptic-like varicosities that are capable of forming functional synapses with rodent myotubes[73], release ACh upon stimulation via exocytosis[74] and contain the essential features of presynaptic elements such as voltage-gated Ca^{2+} channels, IP_3 and ryanodine receptors that activate ER calcium stores, synaptic vesicles and mitochondria[75]. In addition this cell line expresses $5HT_3$ receptors in both the varicosities and soma, but critically do not express functional nAChR[76], thus allowing transient expression of defined exogenous nAChRs in a controlled manner via plasmid transfection, which we have previously shown provides significant expression of functional receptors in the varicosities[67].

All Aβ preparations (including fragments and mutations) were made from purchased lyophilized synthetic product, initially solubilized in ddH_2O and then diluted in a balanced saline solution buffered to pH 7.4.

5. Summary & Significance

Despite the discovery of the presence of high levels of soluble Aβ being strongly correlated with synaptic impairment and loss in AD[77,78], the functional significance of the presence of lower levels (estimated ~200pM) of Aβ in brains of healthy and cognitively normal adults has not been elucidated. However, the facts that it has a remarkably high turnover rate of between 7-8% per hour[79] and its production is regulated by synaptic acitvity[41] strongly indicate that physiological role exists, and its release from the presynaptic terminal[80] indicates that such a role would occur in the synaptic locale.

Findings that not only did picomolar levels of $A\beta_{1-42}$ increase hippocampal long-term potentiation *in vitro* but also enhanced contextual fear memory[21] indicate that the physiological role for Aβ may be as a neuromodulator. It has also shown that the pathway by which Aβ acts as a neuromodulator appears to involve α7-nAChR and that endogenous Aβ is necessary for hippocampal synaptic plasticity, and its related memory mechanisms, and that this effect is due to alterations in presynaptic release frequency[46]. Even more evidence supporting this proposition comes from data that show synaptic transmission decreases in mice with abnormally low levels of Aβ[47].

The presence of high levels of a variety of N-terminal Aβ fragments within the CSF of normal individuals[25] and the discovery of the pathways through which they can be created and regulated[37] coupled with our preliminary findings of the high potency of one of these fragments in activating α7-nAChR indicates that these fragments may play a significant role in neuromodulation. Alteration in the levels of the Aβ fragments during AD may significantly contribute to synaptic disruption seen as an early event in the course of this devastating disease.

Chapter 2

Characterization of the functional activity of N-terminal Aβ fragments and their structural determinants

1. Introduction

Aβ peptides of between 38 and 43 amino acids in length are cleaved from APP by the sequential action of β- then γ-secretase, with $A\beta_{1-42}$ proving to be the dominant toxic species found in fibrillar form in neuritic plaques in the brain[81]. APP is broadly expressed in the brain but is targeted to synapses[22,82]. This results in Aβ being released into the synaptic environment in an nerve activity-dependent manner[41,42]. APP cleavage can also be achieved by sequential cleavage of α- followed by γ-secretase, which yields a different array of peptides [e.g. P3 and sAPPα], with this pathway being described as the alternative or nonamyloidogenic pathway[83,84]. Initial evidence appeared to indicate that the two pathways were mutually exclusive[29,85], however a third pathway has been recently proposed which involves the successive action of α- and β-secretases[37]. This pathway was inferred following the discovery of $A\beta_{1-15}$ and $A\beta_{1-16}$ as being prominent N-terminal Aβ fragments in brain and CSF of both healthy and demented individuals by Portelius et al[86,87]. It was also found that under conditions of reduced γ-secretase activity, this third pathway appears to arise due to an increase in α-secretase activity[37,88], which yield multiple N-terminal Aβ peptide fragments that perhaps coexist at varying levels with $A\beta_{1-42}$. The production of these N-terminal Aβ fragments may be a dynamic physiological event, as there are multiple receptor-linked means by which α-secretase activity may be regulated (e.g. protein kinase C[85]).

$A\beta_{1-42}$ has a domain from the extracellular domain of APP, consisting of 28 amino acids at its N-terminal, whose residues are largely hydrophilic in nature; $A\beta_{1-42}$ also 14 amino acids at its C-terminal from the predicted TM domain of APP, consisting of largely hydrophobic residues. It is therefore likely that these two domains will have different molecular targets, and the N-terminal fragments may represent highly soluble, active peptides.

To date several molecular targets for soluble Aβ have been identified[89]. Two of those targets found at the synapse are nAChR[66,90,91] and certain metabotropic glutamate receptors[48] and both of these types of receptors have been shown to be functionally regulated by Aβ. An agonist-like action of Aβ on presynaptic nAChRs has been previously reported[67,92,93], regulating synaptic plasticity[21,46]. We have recently determined that the activation by Aβ of α7-nAChR occurs via the receptor's agonist-binding domain[56]. To investigate whether these N-terminal Aβ fragments, arising from the aforementioned third pathway, retained the agonist-like activity of Aβ, we examined their impacts on presynaptic Ca^{2+}, post-tetanic potentiation (PTP), long-term potentiation (LTP), and contextual fear conditioning and compared these results to a variety of mutations and truncations of Aβ and N-terminal Aβ fragments.

2. Materials and methods

2.1 *Cell culture*

NG108-15 hybrid neuroblastoma cells were passaged and then plated onto Cell-Tak-coated cover-slips (Warner 15mm, #1) in 35mm dishes containing 15% fetal bovine serum (FBS), 4mM L-glutamine, 0.1mM hypoxanthine-aminopterin-thymidine (HAT), 1% penicillin-streptomycin in Dulbecco's Modified Eagle's Medium (DMEM). Two hours later, the medium was replaced with differentiation medium containing 1% FBS and 1mM db-cAMP in DMEM, and the cells were allowed to differentiate for 48h, during which time they elaborate neurites containing presynaptic-like varicosities.

2.2 *Transfection*

Forty-eight hours post-differentiation, a pcDNA3.1 expression vector containing the mouse α7-nAChR sequence (courtesy of Dr. Jerry Stitzel, University of Colorado) was transiently transfected into the cells using Neuromag (Oz Biosciences), a neuron specific magnetofection transfection reagent that forms non-covalent complexes with nucleic acids, that were then drawn through the plasma membrane with a powerful magnet.

2.3 *Time-series confocal imaging*

Forty-eight hours post-transfection the differentiation medium was removed from the cells and they were then loaded with 5µM Fluo-4 (Invitrogen), a fluorescent Ca^{2+} indicator dye, in an O_2-saturated HEPES-buffered saline solution containing 142mM NaCl, 2.4mM KCl, 1.2mM K_2HPO_4, 1mM $MgCl_2$, 1mM $CaCl_2$, 5mM D-Glucose & 10mM HEPES at pH 7.4 (HBS) for 45min at $37^{O}C$. Cells were then washed with HBS containing 100nM of the Na^+ channel blocker tetrodotoxin (TTX) (HBST) and mounted into a rapid-

exchange Warner open perfusion chamber, which was then secured onto the stage of a Zeiss Axiovert 200M or a Nikon PCM 2000. Perfusion at 3.5mL/min of HBST was started to establish a baseline and imaging was commenced with excitation through 488nm laser and emission filtered through 515-565nm band-pass filter using a 40X/1.3 NA epifluorescence oil-immersion Plan-Neofluar objective. Images were captured every 5s for a total of 30 images via the Zeiss LSM 5 Pascal Imaging System or the Nikon Simple PCI system, with a baseline of 6 images being taken before rapidly switching to the reagent under examination using the Warner six-channel valve-controlled perfusion system.

2.4 *Synaptosome preparation*

Eight-to ten-week-old C57Bl/6J mice (Jackson) were subject to cervical dislocation and immediately decapitated (per Dr. Nichols' approved IACUC protocol). Brains were removed into ice-cold 0.32M sucrose / 1mM EDTA solution (Sucrose Solution), the hippocampi dissected out, and homogenized with a wide-clearance Teflon pestle. The homogenate was then centrifuged at 4,700 rpm for 2min, after which the supernatant was removed and the pellet containing nuclei and cell debris was discarded. The supernatant was then centrifuged at 11,000rpm for 12min and the supernatant discarded; the remaining pellet containing myelin, synaptosomes and mitochondria was resuspended in fresh Sucrose Solution and gently poured onto Percoll density gradients (3%, 10% & 23%), which were centrifuged at 16,500rpm for 5min. Synaptosomes were then removed from between the 10% & 23% Percoll layers via careful pipette evacuation and placed in ice-cold oxygenated HBS and centrifuged at 15,000rpm for 8min, before being washed with oxygenated HBS one more time and spun at 7000rpm for a further 7min. The final synaptosome preparation was stored on ice as a wet pellet until use.

2.5 *Electrophysiology*

Two- to five-month-old C57Bl/6J mice (The Jackson Laboratory) or five- to six-month-old APPswe (Tg2576) and B6/SJL (control littermates) mice (Taconic Biosciences) were anesthetized with tribromoethanol and decapitated (per Dr. Bellinger's approved IACUC protocol). Brains were removed and the hippocampi dissected into ice-cold artificial CSF (aCSF) (containing: 130mM NaCl, 3.5mM KCl, 1.5mM $MgSO_4$, 2mM $CaCl_2$, 1.25mM NaH_2PO_4, 24mM $NaHCO_3$ and 10mM glucose, bubbled with 95% O_2 / 5% CO_2) and slices were cut transversely at 350µm using a vibrating microtome (Leica). Following preincubation at room temperature for 30min, slices are placed in a chamber held at 32°C for a further 30min prior to commencement of recording. Slices were stimulated with 3V at 0.1Hz via a bipolar stimulating electrode placed in the Schaffer collaterals region and population excitatory postsynaptic potentials (pEPSPs) were recorded downstream in the CA1 stratum radiatum region with a 1-5MΩ glass recording electrode filled with 3M NaCl. Stable baseline recordings are recorded for 20min and then long-term potentiation (LTP) is induced via stimulation of the Schaffer collaterals via a theta burst protocol[21] (TBP) (3 x 10-burst trains separated by 15s; a burst = 4 pulses at 100Hz; a train = bursts repeated at 5Hz), recorded in the CA1 stratum radiatum as changes in extracellular field potentials (fEPSP). For Aβ- or Aβ fragment-treated samples, baselines are taken first with aCSF for 15min and then with peptide perfusion for a further 20min, prior to switching back to aCSF and commencement of LTP induction. PTP was recorded in response to the TBP in separate experiments.

2.6 *Contextual Fear conditioning*

C57Bl/6J mice were acclimatized to the animal facility, then deeply anesthetized (1.2% avertin) and cannulae were stereotaxically inserted bilaterally into the dorsal hippocampi using the following coordinates (anteriorposterior = -1.5mm; lateral = ±1mm; depth = -2mm) (per Dr. Todorovic's approved

IACUC protocol). Cannulated mice were then allowed to recover for at least 7 days. pM or nM Aβ or N-terminal Aβ fragment was bilaterally administered via a microinjector into the cannulae over 30s, yielding a maximum volume of 25µL injected into each side. Single-trial contextual conditioning was then performed, consisting of 180s exposure to the conditioning context immediately followed by a mild foot-shock (0.8mA) for 2s. Twenty-four hours later, retention of context-related fear memory was measured by freezing response (considered lack of movement observed at 10s intervals) to re-exposure to the conditioning context. Mean activity during conditioning, activity burst produced by the shock and mean activity during testing in the conditioned context were all automatically measured using a computer-controlled fear conditioning system (TSE Systems). When testing for the specificity of responses to α7-nAChR, 20µM methyllycaconitine (MLA) was bilaterally injected into the dorsal hippocampi alone or just prior to the injection of the Aβ peptides and fear conditioning assessed as above.

2.7 *Western Blotting*

Samples were diluted with SDS-sample buffer and boiled at 90°C for 5min, cooled on ice and spun down before being loaded in 4-20% Tris-HCl or 10-20% Tris-tricine gels (BioRad) and subjected to SDS- or native PAGE. For non-gradient 20% gels and native (non-SDS containing polyacrylamide) gels, the boiling step was skipped. Proteins were then be transferred onto a nitrocellulose or PVDF membrane before blocking with LICOR Odyssey Blocking buffer and overnight incubation with affinity-purified primary antibodies (usually 1:1000). LICOR IRDye anti-rabbit or anti-mouse secondary antibodies were used for detection (usually 1:5000) and imaged on the LICOR Odyssey imager with any quantification being assessed with Image Studio 2.1 software.

2.8 *Coomassie staining*

Following gel electrophoresis, the gel was washed 3 times in ddH_2O for 5min each and soaked in LabSafe Gel Blue™ (Biosciences) for 1h, before washing 3 more times in ddH_2O.

2.9 *Isolation of Aβ fragment oligomers*

Fractionation was achieved via successive membrane ultrafiltration steps using increasing size-cutoff units (e.g. Amicon Ultra centrifugal filter units (Millipore) at 3, 10, 30 kDa cutoffs) at 4000 x *g* for 45mins, providing high speed and high recovery.

2.10 *Chemicals and Aβ preparation*

The following Aβ peptides, fragments and mutants were all purchased from American Peptide (all are human sequences unless otherwise noted): $A\beta_{1-42}$; $A\beta_{42-1}$; $A\beta_{1-15}$; $A\beta_{1-16}$; $A\beta_{1-28}$; $A\beta_{17-42}$; $A\beta_{33-42}$; $A\beta_{1-11}$; [H13A] $A\beta_{1-42}$ and rodent $A\beta_{1-42}$. In addition the following truncated sequences were purchased from Anaspec: $A\beta_{1-9}$; $A\beta_{4-10}$; $A\beta_{1-12}$; $A\beta_{1-13}$ and $A\beta_{1-14}$. Finally the following Aβ fragments and mutants were synthesized by Peptide 2.0: $A\beta_{10-15}$; $A\beta_{15-1}$; [F4A] $A\beta_{1-15}$; [R5A] $A\beta_{1-15}$; [H6A] $A\beta_{1-15}$; [D7A] $A\beta_{1-15}$; [H13A][H14A] $A\beta_{1-15}$ and rodent $A\beta_{1-15}$. Purity of all peptides is confirmed using MALDI-TOF mass spectrometry by Peptide 2.0 and/or the Proteomics Core facility at UH Manoa. Stock solutions were prepared at 0.1-2mM by dissolving the lyophilized synthetic peptides in ddH_2O and stored at -20°C. For use, the peptides were diluted to the required concentration in oxygenated HBS and vortexed to ensure full suspension. Unless otherwise noted, all standard chemicals were obtained from ThermoFisher or Sigma.

2.11 *Statistical analysis*

Each experiment was replicated at least three times. Multiple groups were compared by one-way ANOVA with posthoc Bonferroni multiple comparison test. For comparison of two groups only two-tailed Student t-tests were used. $P<0.05$ was used at the minimal threshold for significance.

3. Results

3.1 *The functional domain for activation of α7-nAChRs by Aβ lies within the first 15 residues*

Having established that the tyrosine at position 188 in α7-nAChRs was essential for receptor activation by $A\beta_{1-42}$ [56], my colleague Dr. Mei Tong started, and then I repeated and continued, the search for the essential residues by initially comparing the effects of a variety of fragments from both the hydrophilic and hydrophobic domains of Aβ on relative changes in Ca^{2+} in NG108-15 cells transfected with α7-nAChR.

The relative changes in Ca^{2+} were assessed in individual presynaptic-like varicosities by measuring the changes in fluorescent intensities (F/F_0) of the Ca^{2+} sensing dye Fluo-4 every 5 s for 30 frames using confocal imaging[67] an example of which is shown in Figure 7A.

We considered two fragments from the hydrophilic domain, $A\beta_{1-15}$ and $A\beta_{1-28}$, the former representing the fragment produced by sequential cleavage of Aβ by the sequential cleavage of α- and β-secretases followed by carboxypeptidase cleavage of the final lysine[37], and the latter being the entire hydrophilic domain. We also considered two fragments from the hydrophobic domain, $A\beta_{17-42}$ and $A\beta_{33-42}$, the former being the P3 fragment and the latter representing the core hydrophobic domain. Both the fragments from the hydrophobic domain essentially lost their agonist-like activity in increasing Ca^{2+}, displaying no significant activity over that found for the control $A\beta_{42-1}$ peptide (39 ± 7% of $A\beta_{1-42}$, n = 32 for $A\beta_{17-42}$; 33 ± 13% of $A\beta_{1-42}$, n = 24 for $A\beta_{33-42}$). However, bearing in mind the assumed cation-π interaction at the active site of α7-nAChR, it was unsurprising that both $A\beta_{1-28}$ and $A\beta_{1-15}$ retained the

same agonist-like activity as $A\beta_{1-42}$, but it was intriguing that $A\beta_{1-15}$ showed a marked increase in activity (157 ± 23% of $A\beta_{1-42}$, n = 29)(Fig. 1C). The reverse sequence of $A\beta_{15-1}$ was also used as additional control (30 ± 10% of $A\beta_{1-42}$; n = 38) which displayed a similar lack of activity over baseline as $A\beta_{42-1}$ and $A\beta_{1-42}$ with mock transfected cells[67].

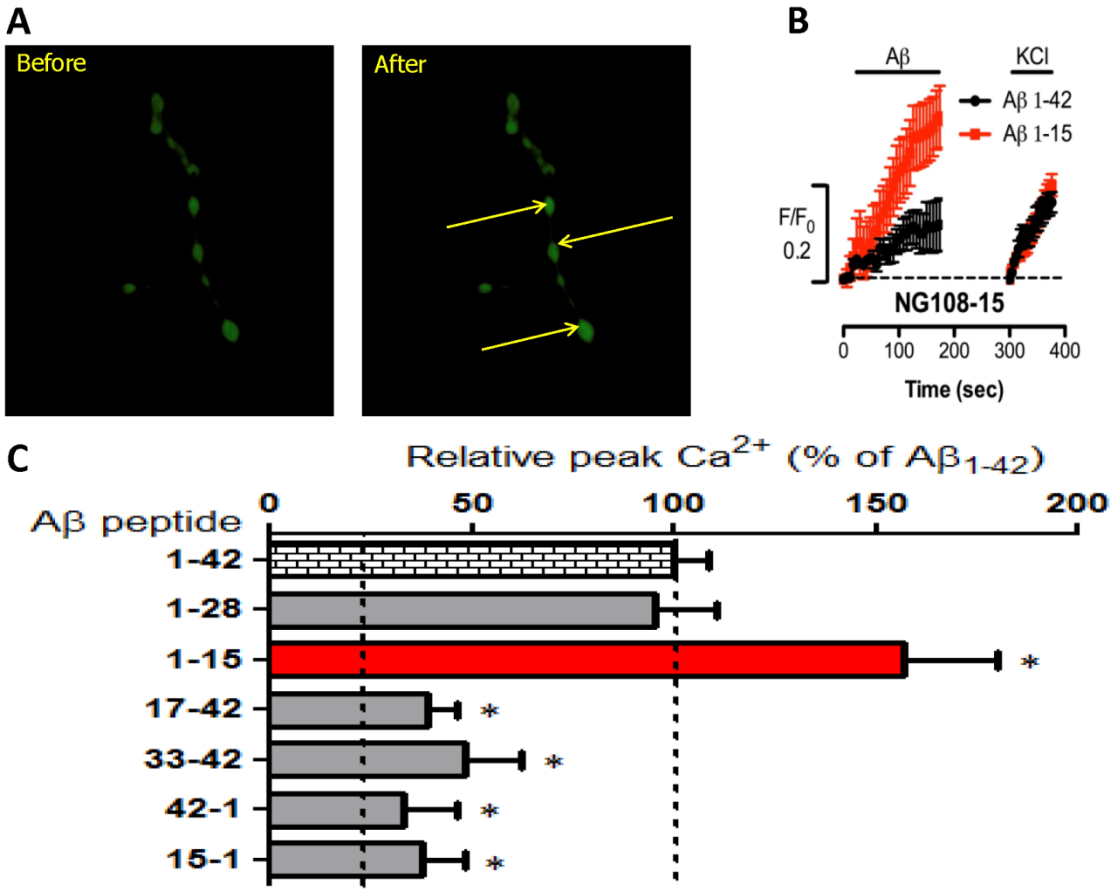

Figure 7. Ca^{2+} responses to Aβ in varicosities of α7-nAChR-transfected NG108-15 cells.

(A) Images of t_0 (Before) & t_{145s} (After) of $A\beta_{1-15}$ perfused cells, some varicosities are marked by arrows. **(B)** Comparison between averaged responses to perfusion with 100nM $A\beta_{1-42}$ (n = 49) and $A\beta_{1-15}$ (n = 178) and later perfusion with elevated KCl to control for cell viability through K^+ depolarization. Time series traces are means ± SEM at individual time points. **(C)** Averaged peak Ca^{2+} responses to 100nM $A\beta_{1-42}$ (n = 44), $A\beta_{1-28}$ (n = 10), $A\beta_{1-15}$ (n = 29), $A\beta_{17-42}$ (n = 32), and $A\beta_{33-42}$ (n = 24), and the control peptides $A\beta_{42-1}$ (n = 24) and $A\beta_{15-1}$ (n = 38). *$p < 0.05$ (Bonferroni *post hoc* tests) NB. Dashed lines indicate baseline (background) and average maximal responses for $A\beta_{1-42}$.

3.2 *The N-terminal fragment is more potent than full length Aβ throughout a wide range of concentrations*

Having discovered the significant increase in agonist-like activity of $A\beta_{1-15}$ over that found for $A\beta_{1-42}$, we confirmed that this activity was not restricted to α7-nAChRs, as the activity was maintained at the same level for α4β2-nAChRs (Fig. 8A).

The potential of this N-terminal fragment perhaps being an endogenous neuromodulator was increased when the experiments were repeated with varying concentrations of $A\beta_{1-42}$ and $A\beta_{1-15}$ which revealed that the $A\beta_{1-15}$ fragment maintained its increased activity compared to $A\beta_{1-42}$ down to 100fM, and had a half maximal effective concentration (EC_{50}) of ≤ 1pM as shown in Figure 8B.

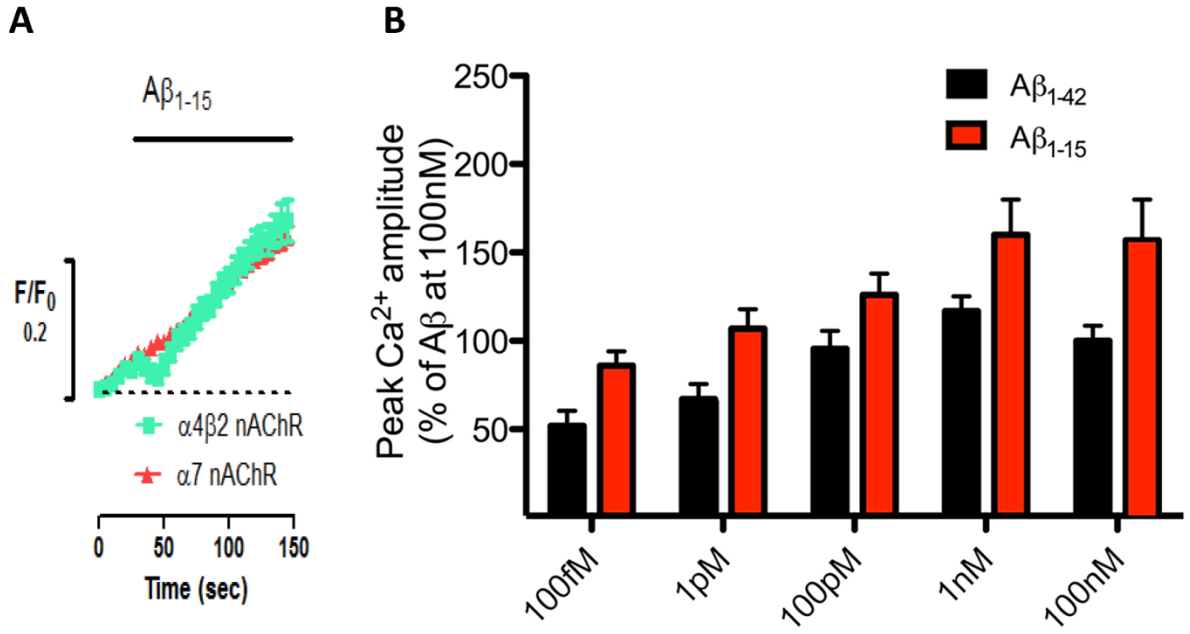

Figure 8. Comparisons of α4β2 and α7 nAChR responses; dose responses of $A\beta_{1-15}$ and $A\beta_{1-42}$

(A) Comparison between averaged responses in varicosities expressing α7-nAChRs (n = 178) or expressing α4β2-nAChRs (n = 17) to perfusion with 100nM $A\beta_{1-15}$. Time series traces are means ± SEM at individual time points. **(B)** Averaged peak Ca^{2+} responses in varicosities expressing α7-nAChRs to: 100fM (n = 22 or n = 33), 1pM (n = 26 or n = 21), 100pM (n = 19 or n = 32), 1nM (n = 30 or n = 15) and 100nM (n = 44 or n = 29) $A\beta_{1-42}$ and $A\beta_{1-15}$

3.3 *The agonist-like action of the N-terminal fragments directly involves activation of nAChRs*

To confirm that the Ca^{2+} changes were induced through the interaction of the N-terminal fragments and nAChRs, as had been found for $A\beta_{1-42}$[56], we perfused $A\beta_{1-15}$ after pre-treatment with the high affinity selective α7-nAChR antagonist αBgTx. In addition, we showed that the specific sequences of $A\beta_{1-15}$ and $A\beta_{1-28}$ interacted and the tyrosine residue at position 188 in the binding pocket of α7-nAChR by either perfusing $A\beta_{1-15}$ or $A\beta_{1-28}$ onto α7-nAChR mutant Y188S transfected cells. All of these treatments resulted in minimal activity as shown in Figure 9.

To seek and explanation for the increase in agonist-like activity of $A\beta_{1-15}$ over that found for $A\beta_{1-42}$, we examined the effect of disrupting the hairpin structure of $A\beta_{1-42}$ by mutating the glutamate located as position 22 of the full length peptide[71]. The relatively conservative substitution of E22Q did not show a significant alteration in activity; however the non-conservative substitution of E22G did significantly reduce the agonist-like activity (Fig. 9). These data indicates that the activity of the $A\beta_{1-15}$ sequence within $A\beta_{1-42}$ is affected by the structure of the full-length peptide.

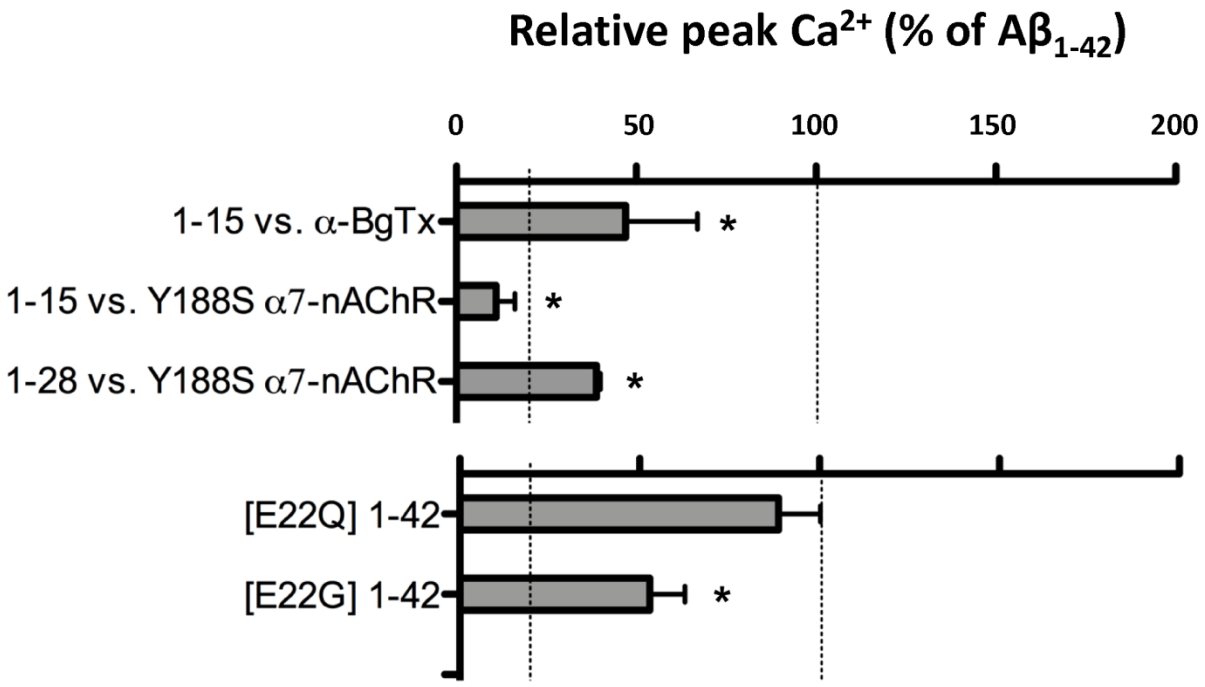

Figure 9. Average peak Ca^{2+} responses in varicosities of NG108-15 cells expressing α7-nAChR to 100nM: $A\beta_{1-15}$ in the presence of 50nM αBgTx (n=12), $A\beta_{1-15}$ on Y188S α7-nAChR (n=20), $A\beta_{1-28}$ on Y188S α7-nAChR (n=11). Peak Ca^{2+} responses to E22Q $A\beta_{1-42}$ (n = 29) and E22G $A\beta_{1-42}$ (n = 19). *$p < 0.05$ (Bonferroni *post hoc* tests) NB. Dashed lines indicate baseline (background) and average maximal responses for $A\beta_{1-42}$.

3.4 *The key amino acids for activation of α7-nAChRs by the N-terminal fragments of Aβ are located in the fragment's C-terminal region*

Having established that the amino acid sequence responsible for the activity of $A\beta_{1-42}$ lay within the N-terminal fragment $A\beta_{1-15}$, we proceeded to attempt to elucidate the precise structural determinants for such activity by examining the activity of an array of sequence mutants and truncations in our *in vitro* presynaptic nerve model.

We commenced by creating alanine mutants of the residues on the N-terminus of $A\beta_{1-15}$ based on the binding of α-bungarotoxin to α1-nAChRs[69]; but also the work of my colleague Dr. Mei Tong[56].

The rodent sequence of $A\beta_{1-42}$ differs from the human one only within the first 13 residues, as shown in Figure 10, and the finding that there was no significant difference between the agonist-like activity of the rodent $A\beta_{1-15}$ fragment as compared to the human $A\beta_{1-15}$ fragment. Although these essentially eliminated the arginine, tyrosine and histidine residues at positions 5, 10 & 13, respectively, as key residues, it is to be noted that the substitutions in the rodent sequence of Y10F and H13R are largely conservative as Y10F retains a benzyl side chain and H13R retains a large basic residue. The elimination of arginine-5 was confirmed using the human $A\beta_{1-15}$ mutant R5A, which also remained active (Fig. 10).

Mutating the very hydrophobic phenylalanine at position 4 indicated a trend to an increase in activity, whereas mutation of the histidine at position 6 showed a trend to decreasing activity, indicating that this residue may be involved in activating α7-nAChR; however, mutating the aspartate at position 7 had no impact (Fig. 10).

Having thus essentially ruled out the most likely candidate residues located at the N-terminus of $A\beta_{1-15}$, we decide to investigate both the activity of the other N-terminal fragments found in human CSF as well as both of the histidine residues located at position 13 and 14 on the C-terminus of $A\beta_{1-15}$.

The alanine mutants of His-13 and His-14 both showed a tendency toward decreased activity compared to $A\beta_{1-15}$, whilst the H13A H14A double mutant showed no significant activity above controls (Fig. 10). The loss of activity being directly related to the removal of these histidines was confirmed by the concomitant loss of activity found in the $A\beta_{1-12}$ fragment. The reduction in activity found with the loss of one of the histidines was also found with $A\beta_{1-13}$, whilst activity was restored in $A\beta_{1-14}$ (Fig. 10). These results showed that both His-13 and His-14 are key to the activity of the N-terminal fragments. Finally, we also confirmed that $A\beta_{1-16}$, being the immediate product of α- and β-secretase cleavage of APP, was also active.

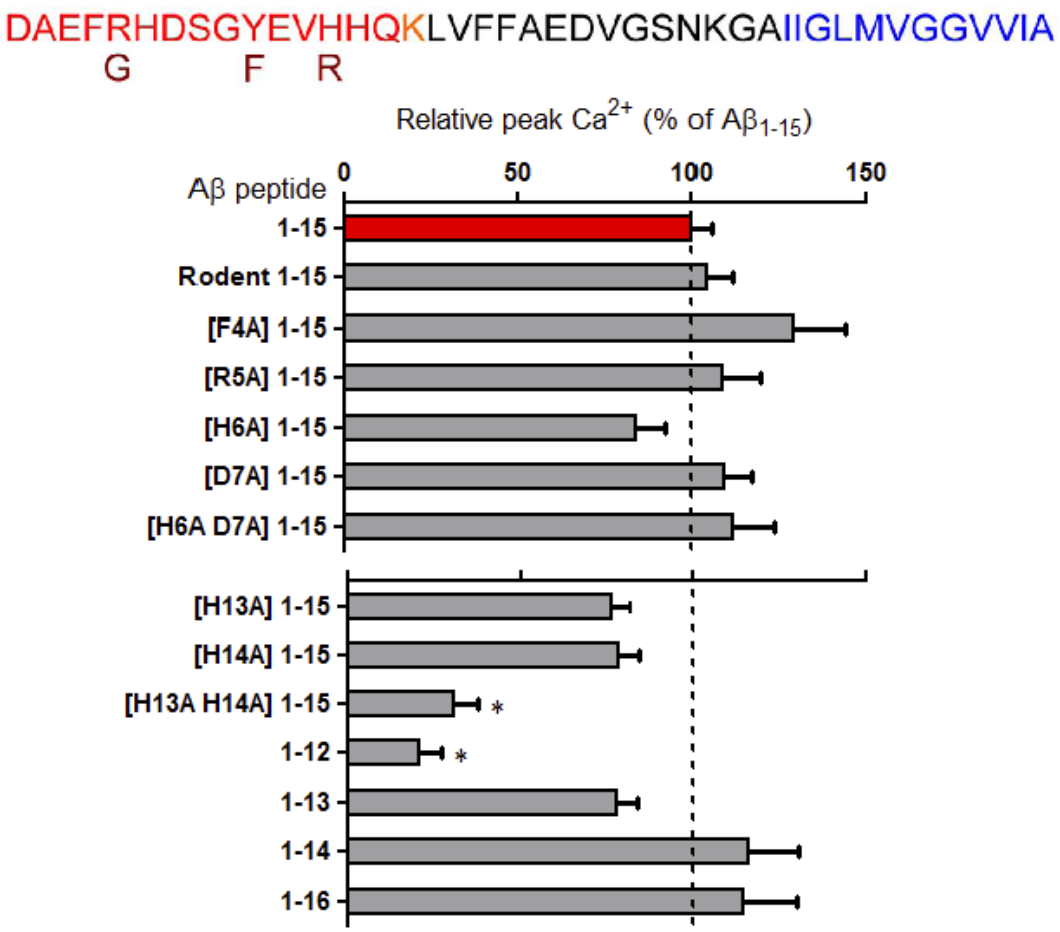

Figure 10. Average peak Ca^{2+} responses in varicosities of NG108-15 cells expressing α7-nAChR to mutants and truncations

(Top) Primary sequence of human $A\beta_{1-42}$ with first 15 residues shown in red and hydrophobic region in blue; the three residues below are the sequence changes found in rodent $A\beta_{1-42}$. (Bottom) Average peak Ca^{2+} responses in varicosities of NG108-15 cells expressing α7-nAChR to 100nM: human $A\beta_{1-15}$ (n = 178), rodent $A\beta_{1-15}$ (n = 39), human $A\beta_{1-15}$ F4A (n = 27), human $A\beta_{1-15}$ R5A (n = 46), human $A\beta_{1-15}$ H6A (n = 34), human $A\beta_{1-15}$ D7A (n = 40), human $A\beta_{1-15}$ H6A D7A (n = 42), human $A\beta_{1-15}$ H13A (n = 24), human $A\beta_{1-15}$ H14A (n = 30), human $A\beta_{1-15}$ H13A H14A (n = 35), human $A\beta_{1-12}$ (n = 48), human $A\beta_{1-13}$ (n = 26), human $A\beta_{1-14}$ (n = 23), human $A\beta_{1-16}$ (n = 51). $^{*}p < 0.05$ (Bonferoni *post hoc* tests) NB. Dashed lines indicate the baseline (background) and average maximal responses for $A\beta_{1-15}$.

3.5 *The N-terminal fragment does not form fibrils nor oligomers and has little secondary structure*

Investigation of the secondary and fibrillar structures that may be involved in the activity of the N-terminal Aβ fragments was commenced by my colleague Dr. Mei Tong, who examined whether $A\beta_{1-15}$ was capable of forming fibrils (or stable aggregates) using Thioflavin-T (ThT) fluorescence. Unlike $A\beta_{1-42}$, the fragment did not display this property (Fig 11A). Our collaborators at the Department of Biochemistry and Molecular Biology at Drexel University College of Medicine, Drs. Mark Contarino and Michael White, sought to discover what, if any, secondary structure exists in soluble $A\beta_{1-15}$ using circular dichroic (CD) spectroscopy. Results showed that there was little organized secondary structure (Fig 11B), as compared to $A\beta_{1-42}$, as evidenced by broad flattening of the spectra.

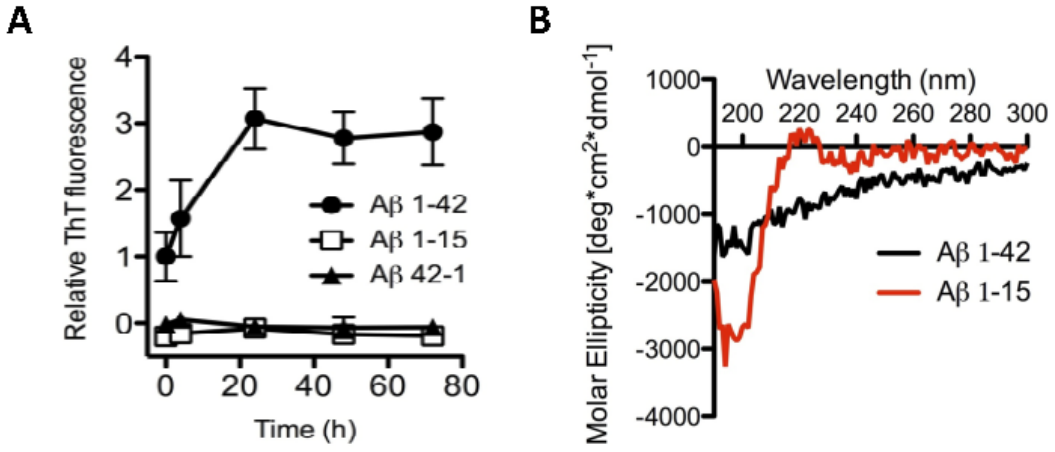

Figure 11. Examination of potential fibrillar and secondary structure

(A) ThT fluorescence for 200nM $A\beta_{1-42}$, $A\beta_{42-1}$ & $A\beta_{1-15}$ (n=3) showing the presence of fibril formation in $A\beta_{1-42}$ only.

(B) Representative CD spectra for $A\beta_{1-42}$ and $A\beta_{1-15}$ with the former indicating β-sheet formation whilst the latter indicating a random secondary structure.

It has been well established that $A\beta_{1-42}$ can form an array of highly stable low-*n* oligomers. To determine the oligomeric state of the N-terminal Aβ fragments examined thus far, we ran 0.1mM samples of our initial $A\beta_{1-15}$ mutations through 4-20% gradient denaturing Tris-HCL SDS-PAGE and then stained gel with the Coomassie-like LabSafe Gel Blue™. The results consistently showed that the majority of the samples running in line with a protein standard in the region of 17kDa, which seemed to imply that they were oligomeric, in the order of decamers to dodecamers (Fig. 12A). There were two exceptions: mutating the arginine at position 5 appeared to eradicate these larger oligomers and mutating the aspartate at position 7 appeared to create two or three bands at even higher oligomeric orders. The effect of mutating the arginine was unexpected given that arginine is normally known to suppress aggregation[94] and was a clue that perhaps these peptides were running anomalously in standard Tris-based SDS polyacrylamide gels.

In contrast, results from PAGE using 10-20% Tris Tricine non-denaturing gels indicated that the N-terminal fragments were, in fact, monomers (data not shown). In order to assess directly the oligomeric status of the fragments, we took two samples of 2nmols of $A\beta_{1-15}$ (molecular weight 1827 Da), passed one through an Amicon 3kDa cutoff filter, which would thus exclude dimers and larger oligomers, and then ran both on a 10-20% Tris-Tricine native gel. The results clearly demonstrated the monomeric status of soluble $A\beta_{1-15}$ (Fig. 12B).

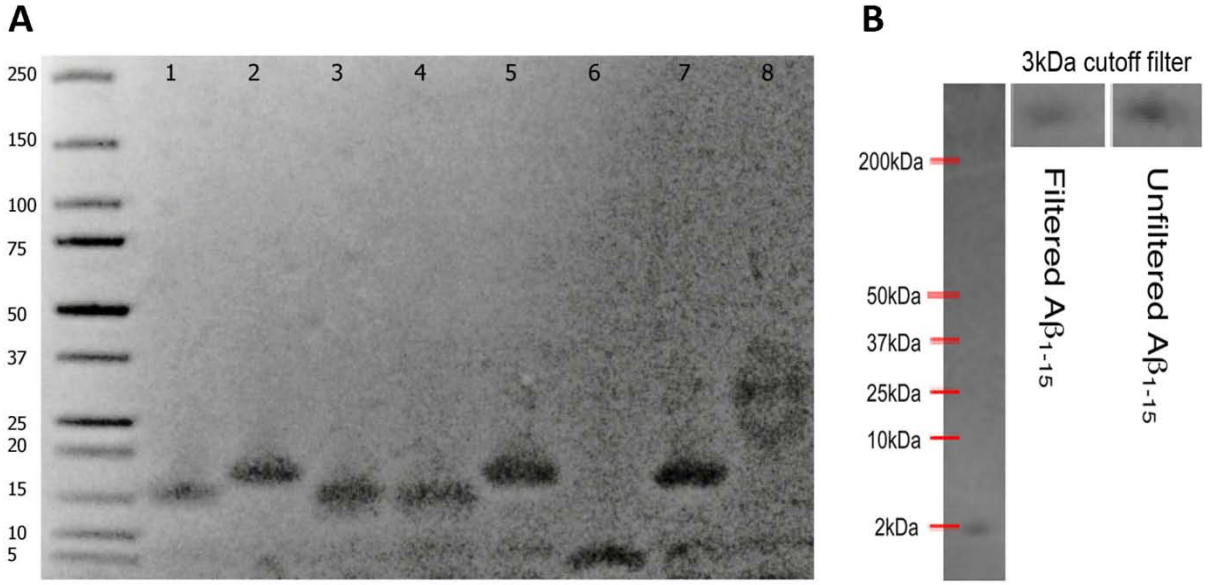

Figure 12. SDS gel analysis of various Aβ fragments

(A) 4-20% gradient denaturing Tris-HCl SDS-PAGE of 1.5nmole of human and rodent $A\beta_{1-15}$, human $A\beta_{1-42}$ and human $A\beta_{1-15}$ alanine substitution mutants, stained with LabSafe Gel Blue. Lanes: 1 = Rodent $A\beta_{1-15}$ (1730 Da), 2 = human $A\beta_{1-15}$ (1827 Da), 3 = human $A\beta_{15-1}$ (1827 Da), 4 = human $A\beta_{1-15}$ scrambled, 5 = human $A\beta_{1-15}$ F4A (1751 Da), 6 = human $A\beta_{1-15}$ R5A (1742 Da), 7 = human $A\beta_{1-15}$ H6A (1762 Da), 8 = human $A\beta_{1-15}$ D7A (1784 Da) (B) 4-20% gradient Tris-Tricine PAGE of 2nmoles of human $A\beta_{1-15}$ (1827 Da), stained with LabSafe Gel Blue. Positions of molecular weight standards (data not shown) are marked in kilodaltons. Insets show a comparison between human $A\beta_{1-15}$ before and after (from whole lane) filtration through an Amicon 3-kDa cutoff filter.

3.6 *The N-terminal fragment is more active than full length Aβ in ex vivo synaptosome model*

Having established the remarkable efficacy of the N-terminal fragment $A\beta_{1-15}$ in the *in vitro* model, we proceeded to test whether this would translate to *ex vivo* models. Firstly, the effect on synaptosomes (isolated presynaptic nerve terminals, which express both α7-nAChRs and α4β2-nAChRs[93]) was examined. The synaptosomes were isolated from the hippocampi of a C57Bl/6J adult mouse via isopycnic centrifugation[95] and loaded with Fluo-4. Efficacy was confirmed as shown in Figure 11.

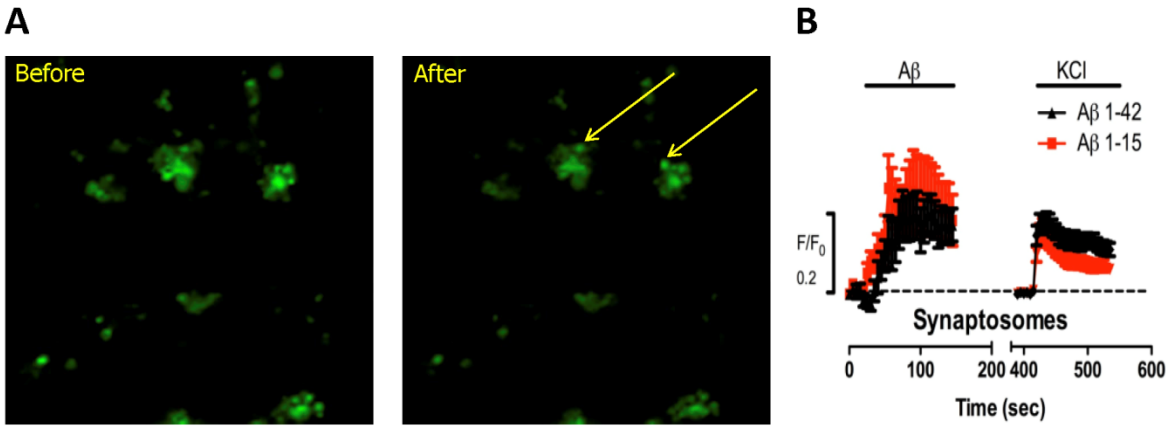

Figure 13. Ca^{2+} responses to Aβ in adult mouse hippocampal synaptosomes

(A) Images of t_0 (Before) & t_{150s} (After) of $A\beta_{1-15}$ perfused synaptosomes preloaded with Fluo-4 with some responding synaptosomes marked by arrows. **(B)** Comparison of responses to 100nM human $A\beta_{1-42}$ (n=16) and human $A\beta_{1-15}$ (n=26), followed by K^+ depolarization. Time series traces are means ± SEM at individual time points.

3.7 *The N-terminal fragment enhances PTP and LTP in hippocampal slices*

Next, we moved to another *ex vivo* model to determine the functional consequence of acute application of $A\beta_{1-15}$ by examining its impact on synaptic plasticity through electrophysiological examination of mouse hippocampal slices. One of the key aspects of synaptic plasticity is LTP, which is the long-lasting enhancement of signal transmission across a synapse and is also thought to be one of the underlying molecular mechanisms involved in learning and memory. My colleague, Naghum Alfulaij, assessed the changes in synaptic plasticity resulting from inducing PTP and LTP via theta-burst stimulation via the Schaffer collaterals, a pattern of firing that mimics physiological patterns recorded *in vivo* during exploratory behavior. As discussed earlier, multiple studies have found that $A\beta_{1-42}$ enhances PTP and LTP at picomolar concentrations[21] yet demonstrates a strong inhibitory effect at high nanomolar or micromolar concentrations[96]. Having first controlled for variations in input/output (Fig. 14A), we found that prior incubation with femtomolar $A\beta_{1-15}$ significantly enhanced PTP (Fig. 14B) and LTP (Fig. 14C & D; peak, 184 ± 25% of baseline; plateau, 162 ± 12% of baseline), without any effect on baseline responses before induction of LTP. We also found that neither picomolar (Fig. 14C) nor nanomolar (data not shown) $A\beta_{1-15}$ had a significant effect on LTP. The lack of effect at picomolar concentration contrasts with the findings for $A\beta_{1-42}$, although appears to be in line with the finding by Portelius et al that a concentration of ~1nM $A\beta_{1-16}$ similarly displayed no significant change in LTP compared to controls[86]. These results indicate the N-terminal domain of Aβ may account for the positive neuromodulatory activity of the full-length peptide[21,46], whilst also highlighting the need to examine further concentrations of $A\beta_{1-15}$.

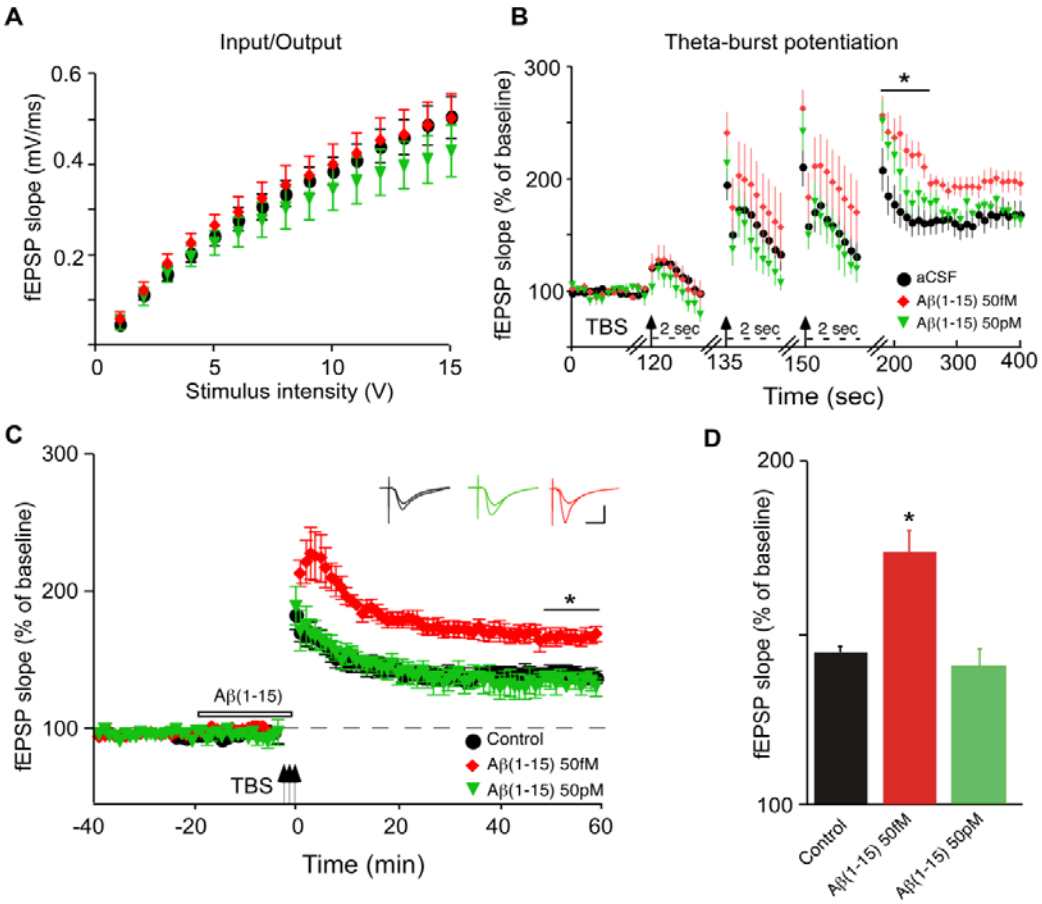

Figure 14. Effects of $A\beta_{1-15}$ PTP and LTP induction

Hippocampal slices were superfused with aCSF containing vehicle (control), 57fM $A\beta_{1-15}$ or 57pM $A\beta_{1-15}$, followed by the induction of LTP in the CA1 region via theta burst stimulation (TBP: four trains of 100 Hz pulses delivered at 5 Hz repeated three times every 15 s for a total of 3 bursts) or HFS (two 1 s trains of 100 Hz separated by 20 s) through the Schaffer collaterals and expressed as normalized fEPSP slope values. (**A)** Control input/output curves, before treatment. **(B)** Recording during and after theta burst following 57 fM or 57 pM $A\beta_{1-15}$ for 20 mins, with the start of each burst marked with an arrow. Note the change in time scale (dashed lines) for the bursts: PTP marked with a solid bar. **(C)** TBP-induced LTP with color-coded insets showing example fEPSPs for control aCSF (black), femtomolar $A\beta_{1-15}$ (red) or picomolar $A\beta_{1-15}$ (green) for baseline and LTP. The period of $A\beta_{1-15}$ pretreatment is marked by the open bar. **(D)** Average fEPSP slope values for the end of the plateau (50-60 min post-tetanus), as noted by the solid bar in **C**(*). Data are the means ±SD, n = 6 slices/group derived from three experiments. Calibration: horizontal, 10ms; vertical, 0.4mV. *$p < 0.05$ (Bonferroni *post hoc* tests).

3.8 *The N-terminal fragment enhances contextual fear conditioning*

The results thus far encouraged us to examine the effects of $A\beta_{1-15}$ on hippocampal-based learning and memory *in vivo*, which was conducted by Drs. Cedomir Todorovic and Tessi Sherrin, Cell & Molecular Biology at UH JABSOM, using an established fear conditioning paradigm[97]. Following recovery from surgery to insert cannulae into the dorsal hippocampi of adult C57Bl/6J mice, $A\beta_{1-42}$, $A\beta_{1-15}$, or physiological saline solution was bilaterally injected. Single-trial contextual fear conditioning was then performed and retention of that fear memory was measured 24 hours later by recording the freezing (lack of movement) response to the conditioned context. Results showed that there was a pronounced enhancement of fear conditioning at 100pM concentrations of $A\beta_{1-15}$, not present at 100nM levels of $A\beta_{1-15}$ and above that found at 100pM levels for $A\beta_{1-42}$. There was no effect of injected $A\beta_{1-15}$ on basal locomotion (as mean activity) either to the new context or shock (data not shown). To further confirm that this effect on contextual fear memory was due to the interaction of $A\beta_{1-15}$ with α7-nAChR, the experiment was repeated with the administration of the selective α7-nAChR blocker MLA, which did indeed attenuate the enhancement (Fig. 15).

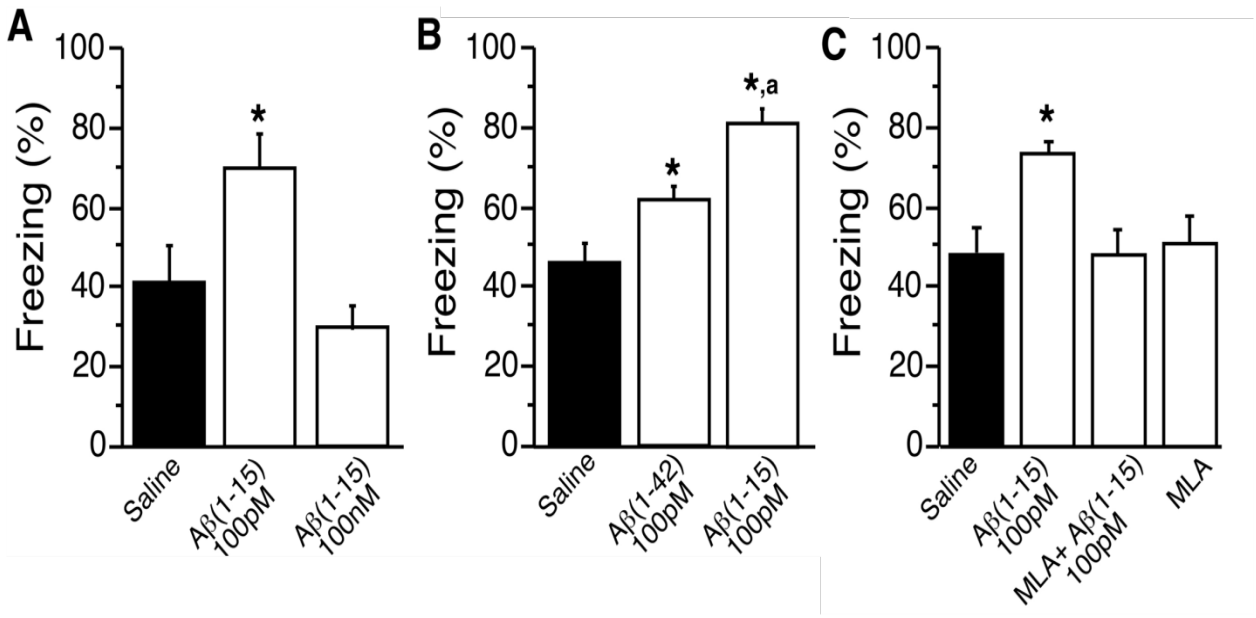

Figure 15. Contextual fear conditioning

Using single-trial paradigm utilizing mild shock after bilateral injection into the dorsal hippocampi of either sterile saline or **(A)** 100pm $A\beta_{1-15}$, 100nM $A\beta_{1-15}$; **(B)** 100pM $A\beta_{1-42}$, 100pM $A\beta_{1-15}$; or **(C)** 100pM $A\beta_{1-15}$, 100pM $A\beta_{1-15}$ + 100nM MLA (nAChR antagonist), 100nM MLA. Freezing to context was assessed 24h later by two trained observers. Baseline freezing was assessed via TSE videotracking software. Data are means ± SEM, (*n* = 6-9 mice/group). [a]P<0.05 comparing $A\beta_{1-15}$ to $A\beta_{1-42}$; * P<0.005 compared to saline control (Bonferroni *post hoc* tests).

3.9 *The N-terminal fragment partially reverses reduced α7-nAChRs responses to full-length Aβ responses*

To evaluate the potential modulatory activity of the N-terminal fragment in the presence of $A\beta_{1-42}$, we tested various mixtures of concentrations of the two peptides using our *in vitro* presynaptic nerve model. For both picomolar and nanomolar concentrations there was no significant effect, but the inclusion of $A\beta_{1-15}$ did show a trend toward increased responses over those observed for $A\beta_{1-42}$ alone (compare Figs. 8B and 16). However, the N-terminal fragment appears to partially reverse the strongly reduced response to $A\beta_{1-42}$ alone for highly elevated levels of $A\beta_{1-42}$ (1μM) (Fig. 16). This result indicated a potential neuromodulatory restorative effect of $A\beta_{1-15}$.

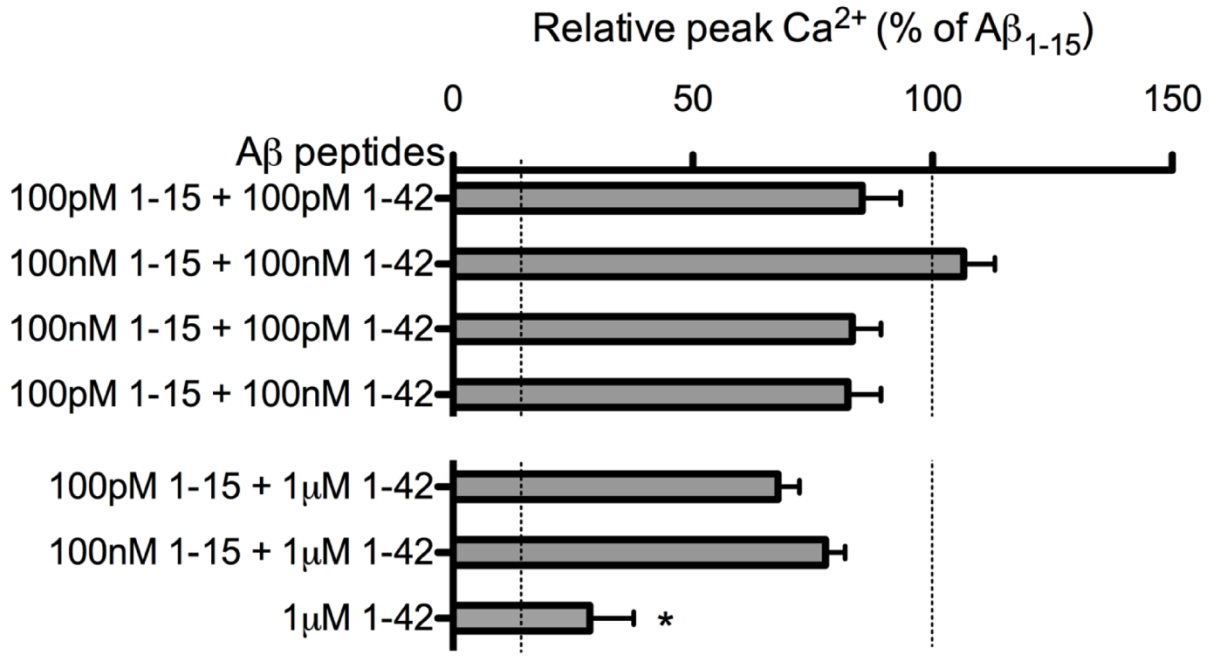

Figure 16. Averaged peak Ca^{2+} responses to mixtures of $A\beta_{1-15}$ and $A\beta_{1-42}$ at various concentrations.

100pM $A\beta_{1-15}$ & $A\beta_{1-42}$ (n = 27), 100nM $A\beta_{1-15}$ & $A\beta_{1-42}$ (n = 28), 100nM $A\beta_{1-15}$ & 100pM $A\beta_{1-42}$ (n = 28), 100pM $A\beta_{1-15}$ & 100nM $A\beta_{1-42}$ (n = 34), 100pM $A\beta_{1-15}$ & 1μM $A\beta_{1-42}$ (n = 33), 100nM $A\beta_{1-15}$ & 1μM $A\beta_{1-42}$ (n = 39), $A\beta_{1-15}$ & $A\beta_{1-42}$ (n = 13). $^{*}p < 0.05$ (Bonferoni *post hoc* tests) NB. Dashed lines indicate the baseline (background) and average maximal responses for $A\beta_{1-15}$.

3.10 *The N-terminal fragment rescues LTP deficits in APPswe mouse hippocampal slices*

To further examine the potential neuromodulatory restorative effect of $A\beta_{1-15}$ *ex vivo*, we decided to directly assess the effects of $A\beta_{1-15}$ on LTP in the context of elevated $A\beta_{1-42}$ which has been shown (at high nanomolar concentrations) to result in inhibition of LTP induced by HFS[98]. Accordingly, hippocampi from wild-type mice were first treated with $A\beta_{1-15}$ or not (control) and then $A\beta_{1-42}$ and then induced LTP as previously described. Results showed that LTP was inhibited by the presence of $A\beta_{1-42}$ alone but the pretreatment of $A\beta_{1-15}$ prevented this impairment (Fig. 17 A & B). These results further indicated that $A\beta_{1-15}$ can function as strong, positive neuromodulator even in the presence of highly elevated levels of $A\beta_{1-42}$.

Next, my colleague examined the effects of pretreatment with $A\beta_{1-15}$ on hippocampi from APPswe mice, which express mutations found in a form of familial Alzheimer's disease whereby a decrement in LTP is found that appears to be largely due to elevated levels of $A\beta_{1-42}$. As with the wild-type, in this model the pretreatment with $A\beta_{1-15}$ led to a full "rescue" of LTP, here induced with high-frequency stimulation (Fig. 17 C & D)

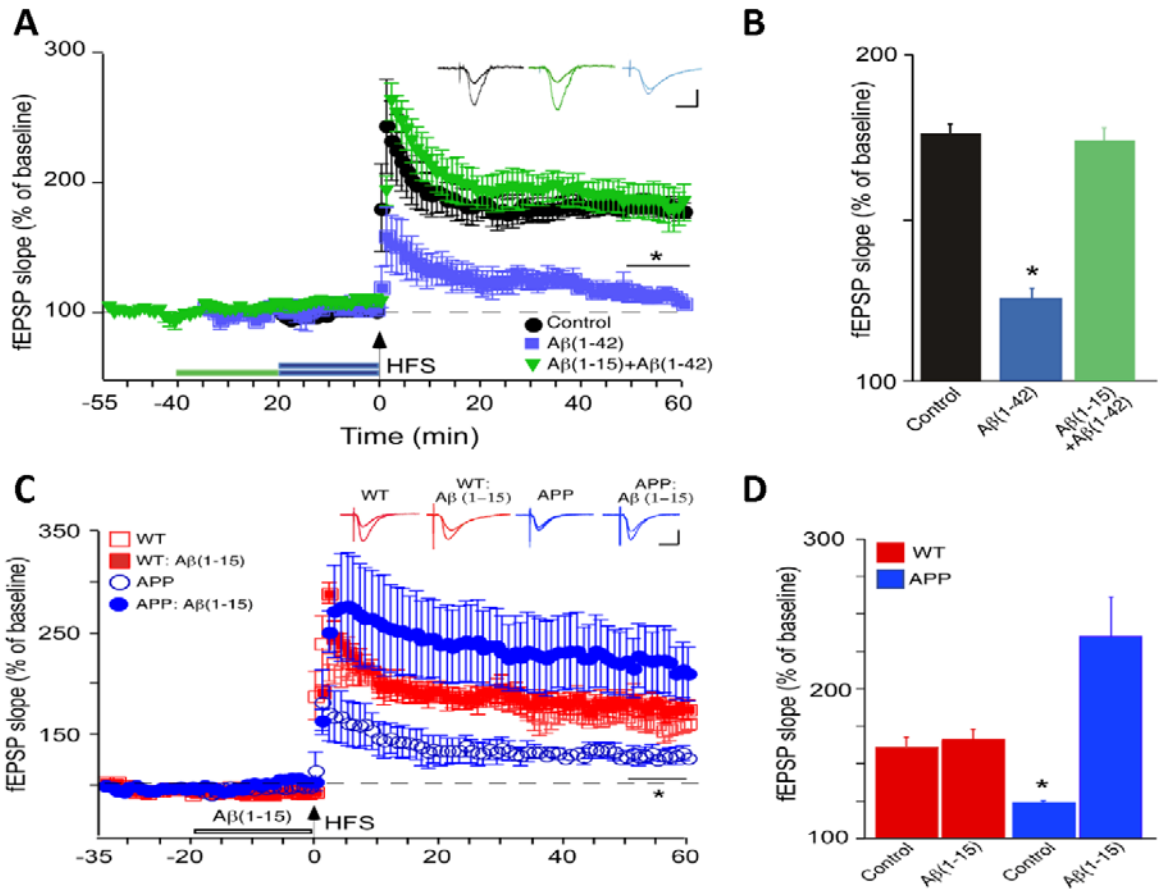

Figure 17. N-terminal fragment rescues LTP deficits resulting from the presence of elevated $A\beta_{1-42}$

(A) HFS-induced LTP, with color-coded insets showing example fEPSPs for control of aCSF (black), 500nM $A\beta_{1-42}$ (blue), or 500nM $A\beta_{1-15}$ followed by 500nM $A\beta_{1-42}$ (green) for baseline and LTP; periods of peptide pretreatment are marked by the bars. **(B)** Average fEPSP slope values for the end of the plateau (50-60 min post-tetanus), as noted by the solid black bar in (A*). **(C & D)** Hippocampal slices from APPswe or wild-type (WT) littermates were superfused with aCSF containing vehicle (Control) or 500nM $A\beta_{1-15}$. **(C)** HFS-induced LTP, with color-coded insets showing example fEPSPs for slices form WT (red) or APPSwe (blue) mice with or without pretreatment with $A\beta_{1-15}$ for baseline and LTP; period of $A\beta_{1-15}$ pretreatment marked by the open bar. **(D)** Average fEPSP slope values for the end of the plateau (50-60 min post-tetanus), as noted by the solid black bar in (C*). Data are the means ± SD,(n = 6 slices/group for A, B) (n = 4 slices/group for C, D) derived from three experiments. Calibration: horizontal 10ms; vertical, 0.4mV. *$p < 0.05$ (Bonferoni *post hoc* test).

4. Discussion

Multiple studies have recently indicated a neuromodulatory role for Aβ at normal picomolar concentrations[21,99], with synaptic function being potentially regulated by both Ca^{2+}-dependent presynaptic neuronal vesicle release[100] and α7 nAChR-dependent Ca^{2+}-induced astrocytic release of glutamate[101]. Our work in Lawrence et al[102] confirms this role and further extends it by identifying the N-terminal hydrophilic region of Aβ responsible for the agonist-like activity of the peptide[56,67] as well as indicating that the N-terminal fragments that result from the action of both α- and β-secretase activity, first described by Portelius et al[37,86–88], could act as highly potent synaptic regulators.

APP cleavage was thought to occur in mutually exclusive pathways by α- and β-secretase; however ADAM10 (constitutive α-secretase) and BACE (β-secretase) have been found to be coordinately expressed in brain[103]. This indicates that there is the potential of some constitutive production of $A\beta_{1-15}$ even at levels of α-secretase activity, which, bearing in mind the potency of this fragment at picomolar or lower concentrations, could significantly regulate synaptic function. Moreover cleavage by ADAM17 (regulated α-secretase) may be activated by one or more receptor pathways[104] indicating that the production of the fragment may be a tightly controlled event. However, the steady-state level of $A\beta_{1-15}$ and other fragments and the extent of either type of α-secretase activity at the synapse is yet to be determined, nor is there any information regarding the activity of the other enzymes involved in the production of the shorter N-terminal fragments (e.g. $A\beta_{1-14}$) found by Portelius et al in CSF[87].

The case for $A\beta_{1-15}$ being a potent synaptic regulator was further enhanced by the results of the synaptic plasticity electrophysiological and fear condition experiments, which again showed the regulation to be concentration-dependent. These data, however, brought forward important questions as to what the

effective endogenous concentrations of Aβ and its fragments might be. Perfusion of soluble proteins over hippocampal slices or via intrahippocampal injections is notorious for the difficulties it creates in discovering their effective concentrations in synaptic locales, primary due to non-specific and off-target binding. In addition, in view of the heterogeneity of the structures in the solubilized form of $A\beta_{1-42}$, it is possible that the effective concentration of the active form is considerably less than previously reported[21,56,92], with some structures restricting access to the histidines at positions 13 and 14, whilst others, notably those in the hydrophobic domain, potentially interacting with other membrane structures.

Moreover, despite our work implicating the involvement of nicotinic receptors in regulating synaptic plasticity and fear conditioning, confirming prior studies' findings[21], it does not exclude the possibility of other receptor targets. Indeed, the inhibitory effect of high nanomolar to micromolar levels of $A\beta_{1-42}$ has been well documented[96] and has suggested that this is a result of entirely separate pathways[105]. It may also be possible that these higher concentrations are merely desensitizing, but elucidation of all of these interactions at the synapse will be important to discover, as well as how they change over the progression of Alzheimer's disease.

The findings that $A\beta_{1-15}$ was incapable of forming fibrils or oligomers, unlike full length Aβ, and was predominantly random in structure in CD spectral analysis indicates that access to its residues is less restricted than it is in $A\beta_{1-42}$. Indeed, previous studies have shown that $A\beta_{1-42}$ consists of a random/weak loop structure from residues 1-14, then a β-strand structure from 15-21, followed by a turn at residue 22 and then another β-strand from 24-30[71]. We postulate therefore that it is this structure (in particular the turn at the glutamate residue at position 22) restricting the availability of the histidines at positions

13 and 14 that is responsible for the decreased agonist-like activity of $A\beta_{1-42}$ and $A\beta_{1-28}$ as compared to $A\beta_{1-15}$.

Our work in both our *in vitro* presynaptic model and electrophysiology experiments also indicated a very intriguing property of the N-terminal fragment, in that it was able to partially reverse reduced agonist-like activity caused by micromolar concentrations of $A\beta_{1-42}$ as well as rescue deficits in LTP caused by high concentrations of exogenous $A\beta_{1-42}$ or those found in APPswe mice. Whether this is through direct competition between the N-terminal fragment and $A\beta_{1-42}$, greater binding affinity with receptors or merely a compensatory higher activity with the receptors to which it does bind is as yet undetermined. However, as earlier studies indicated that the first 28 residues of $A\beta_{1-42}$ do not contribute to its toxicity[106], it is also likely that the N-terminal fragments are also non-toxic, particularly as they do not contain the hydrophobic residues at or near the glycine at position 33, which have been shown to largely account for the toxicity of the full length peptide[107].

The combination of the reduction in negative synaptic effects of $A\beta_{1-42}$ by the N-terminal fragments and the possibility that they may prove to be non-toxic open the door to the possibility that they may have a neuroprotective property in addition to its neuromodulatory one.

Chapter 3

Characterization of the minimum amino acid sequence responsible for the functional activity of the N-terminal Aβ fragment

1. Introduction

Our findings that the key amino acids of $A\beta_{1-42}$ required for activation of α7nAChR are two histidines that reside in the C-terminal region of the N-terminal fragments[102], found to be present in human CSF[87], combined with Tong et al's discovery of a tyrosine residue in α7nAChR essential for that activity[56] begs several questions. Not least of these questions is the part that the surrounding residues of $A\beta_{1-42}$ or its fragments play in either enhancing or hindering that activity.

The interaction between the basic histidine residues of Aβ and the aromatic tyrosine residue of the receptor is likely an attraction between either or both of the protonated imidazole side chain or its π-electrons and the π-electrons of tyrosine's benzyl ring. It is possible therefore that either increasing the positive charge clustered in C-terminal region of the N-terminal fragments or the amount of π-electrons therein, or both, may enhance the interaction and thereby facilitating an increase in agonist-like activity.

It is also possible that the electrostatic properties of the surrounding residues may help to orient the histidines correctly in the binding pocket of α7nAChR and thus affect both the binding and activation qualities of the peptide. Bearing in mind our findings that the N-terminal fragments induce greater levels of agonist-like activity in these receptors that full length Aβ, whilst not forming larger soluble structures than monomers, such interactions are extremely likely. Four of the key residues within the binding site of α7nAChR are tryptophans whilst the other three are tyrosines[54], all of which are aromatic, thus leading to the likelihood any residue within the N-terminal fragment that might assist in the optimal alignment of His-13 and His-14 would again have a small positive charge or also contain π-electrons.

By examining a series of mutant and truncations of the C-terminal region of the N-terminal fragments to investigate the essential properties of the residues in the peptides' active site, we pave the way for the development of potential peptidomimetics that may not only be potent neuromodulators but also provide neuroprotection against the harmful binding of $A\beta_{1-42}$[108] by competitively binding to the receptor.

2. Materials and methods

2.1 *Cell Culture*

As described in Chapter 2

2.2 *Transfection*

As described in Chapter 2

2.3 *Time-Series Confocal Imaging*

As described in Chapter 2

2.4 *Fear Conditioning*

As described in Chapter 2

2.5 *Chemicals and Aβ preparation*

As described in Chapter 2 except for the additional synthesis by Peptide 2.0 of the following mutant and truncated Aβ fragments: Rodent $A\beta_{10-15}$; [F1A] $A\beta_{10-15}$; [E2A] $A\beta_{10-15}$; [V3A] $A\beta_{10-15}$; [H4A] $A\beta_{10-15}$; [Q6A] $A\beta_{10-15}$; [H4R][H5A] $A\beta_{10-15}$; [H4A][H5R] $A\beta_{10-15}$; [H4K][H5A] $A\beta_{10-15}$; [H4A][H5K] $A\beta_{10-15}$; [E2R] $A\beta_{10-15}$; [Q6D] $A\beta_{10-15}$; [Y1S] $A\beta_{10-15}$; [Q6H] $A\beta_{10-15}$; [V3H] $A\beta_{10-15}$; [V3S] $A\beta_{10-15}$; [E2C] $A\beta_{10-15}$; [H4F][H5F] $A\beta_{10-15}$; $A\beta_{11-15}$; $A\beta_{12-15}$; $A\beta_{10-14}$; $A\beta_{11-14}$ and [Y1succinyl] $A\beta_{10-15}$

3. Results

3.1 *Hexameric C-terminal fragment of N-Terminal Aβ fragment is sufficient for activation of α7-nAChRs*

Having established that the essential residues in the C-terminal region of the N-terminal fragment $A\beta_{1-15}$, through mutation and truncations, were His-13 and His-14[102], we examined the hexameric truncation of that region, $A\beta_{10-15}$, and also $A\beta_{12-28}$ (performed by my colleague Dr Mei Tong), which has been previously found to significant agonist-like activity[66,92]. Both fragments were found to retain the agonist-like activity of $A\beta_{1-15}$ (Fig. 18), confirming our earlier findings. There was a trend to a slightly reduced response in $A\beta_{10-15}$ although this was not significant.

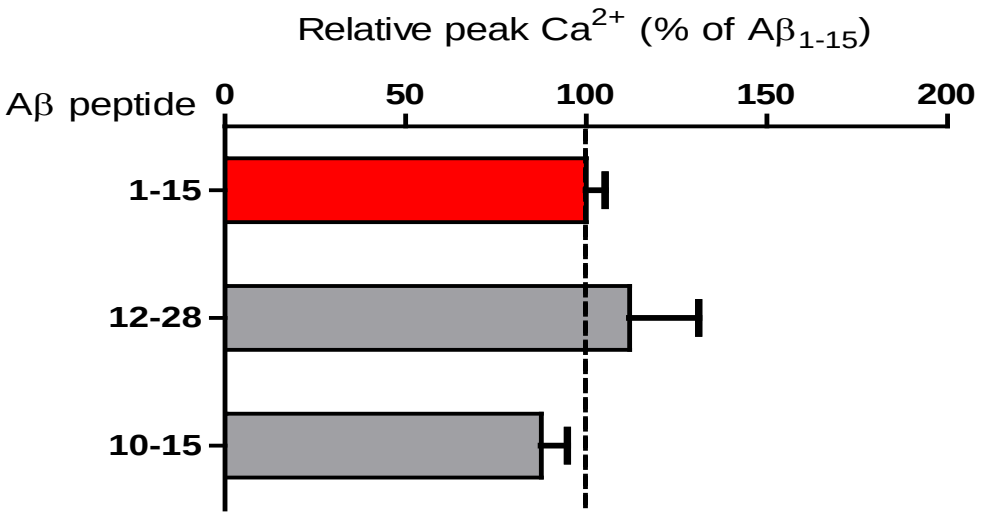

Figure 18. Average peak Ca^{2+} responses in varicosities of NG108-15 cells expressing α7-nAChR to $A\beta_{10-15}$ or $A\beta_{12-28}$

Averaged peak Ca^{2+} responses to 100nM $A\beta_{1-15}$ (n = 178), $A\beta_{12-28}$ (n = 17) and $A\beta_{10-15}$ (n = 29). NB. Dashed line indicates average maximal responses for $A\beta_{1-15}$.

3.2 *Hexameric C-terminal fragment of N-Terminal Aβ fragment enhances contextual fear conditioning*

The results of our *in vitro* model encouraged us to examine whether the agonist-like activity of $A\beta_{10-15}$ found therein had functional implications *in vivo*. Accordingly our collaborators Drs. Cedomir Todorovic and Tessi Sherrin performed the same contextual fear conditioning paradigm as was used in Chapter 2. Results showed a significant increase in freezing (lack of movement) over control (saline 64.5 ± 4%, n = 8; $A\beta_{10-15}$ 83.9 ± 2%, n = 8) indicating that $A\beta_{10-15}$ also remained active *in vivo*.

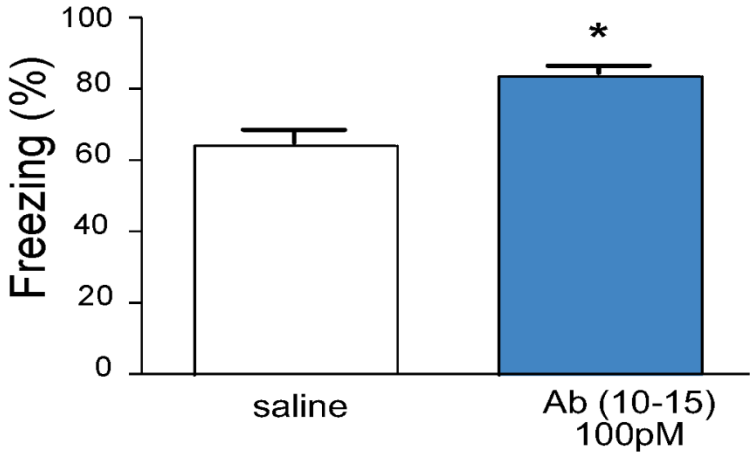

Figure 19. Contextual fear conditioning with $A\beta_{10\text{-}15}$

Single-trial fear conditioning paradigm performed utilizing mild shock after bilateral injection into the dorsal hippocampi of either sterile saline or 100pm $A\beta_{10\text{-}15}$. Freezing to context was assessed 24h later by two trained observers. Baseline freezing was assessed via TSE videotracking software. Data are means ± SEM, (*n* = 8 mice/group). * P<0.005 compared to saline control (Bonferroni *post hoc* tests).

3.3 *Both His-13 and His-14 remain essential in the activity of the hexameric Aβ fragment and Tyr-10 may also play an important role*

Having isolated the agonist-like activity of $A\beta_{1-15}$ to this C-terminal region YEVHHQ ($A\beta_{10-15}$), we proceeded to examine the contribution of each amino acid in this sequence via a series of conservative and non-conservative mutations as well as the effects of further truncations (Fig. 20).

Firstly, we sought to examine the effects of substituting His-13 and His-14 (Fig. 20A). Alanine mutants of both histidines confirmed our previous findings of the essential nature of these residues[102], as activity was essentially lost. The substitution of both histidines with phenylalanines, thus remaining within the aromatic structural class, showed a trend towards reduced activity. The conservative substitutions of either histidine with an arginine or a lysine, with concomitant alanine substitution for the other histidine also showed a trend towards reduced activity; however, none of these substitutions were significant, possibly due to the comparatively low *n*-values for these mutations compared to those for $A\beta_{10-15}$.

To discover what, if any, contribution the remaining residues in $A\beta_{10-15}$ made on the agonist-like activity of $A\beta_{10-15}$, we examined the effect of alanine mutants of each (Fig. 20B). A non-significant trend for reduction in each was found, with the mutation of the tyrosine falling only just short of significance. The trend found for the result for the Y10A substitution, reached significance with the non-conservative substitutions of serine or a succinyl group for Tyr-10, both involving the loss of the benzyl ring (Fig. 20C). This implies that the benzyl ring at Tyr-10 is an important aspect of the activity of $A\beta_{10-15}$, possibly in orienting the histidines into active site of the nAChRs.

The substitution of the acidic glutamate Glu-11 to cysteine, which replaces the hydroxyl in glutamate's carboxyl group with a thiol, showed a non-significant trend in reduced response; however, substituting the basic arginine for acidic Glu-11 produced no change in activity (Fig. 20C). When the hydrophobic valine Val-12 was substituted by a basic histidine or a polar serine, a non-significant trend was found for a reduction in activity (Fig. 20C). Substituting the polar glutamine Glu-15 to an acidic aspartate produced a non-significant trend in reduced activity; whereas substitution of a basic histidine showed an intriguing trend to increasing activity over $A\beta_{10\text{-}15}$ (Fig. 20C).

Results from truncating $A\beta_{10\text{-}15}$ into $A\beta_{10\text{-}14}$, displayed no change in activity, whilst truncations into either $A\beta_{11\text{-}14}$, $A\beta_{11\text{-}15}$, or $A\beta_{12\text{-}15}$ (Fig. 20D) all showed non-significant trends in a reduction of activity.

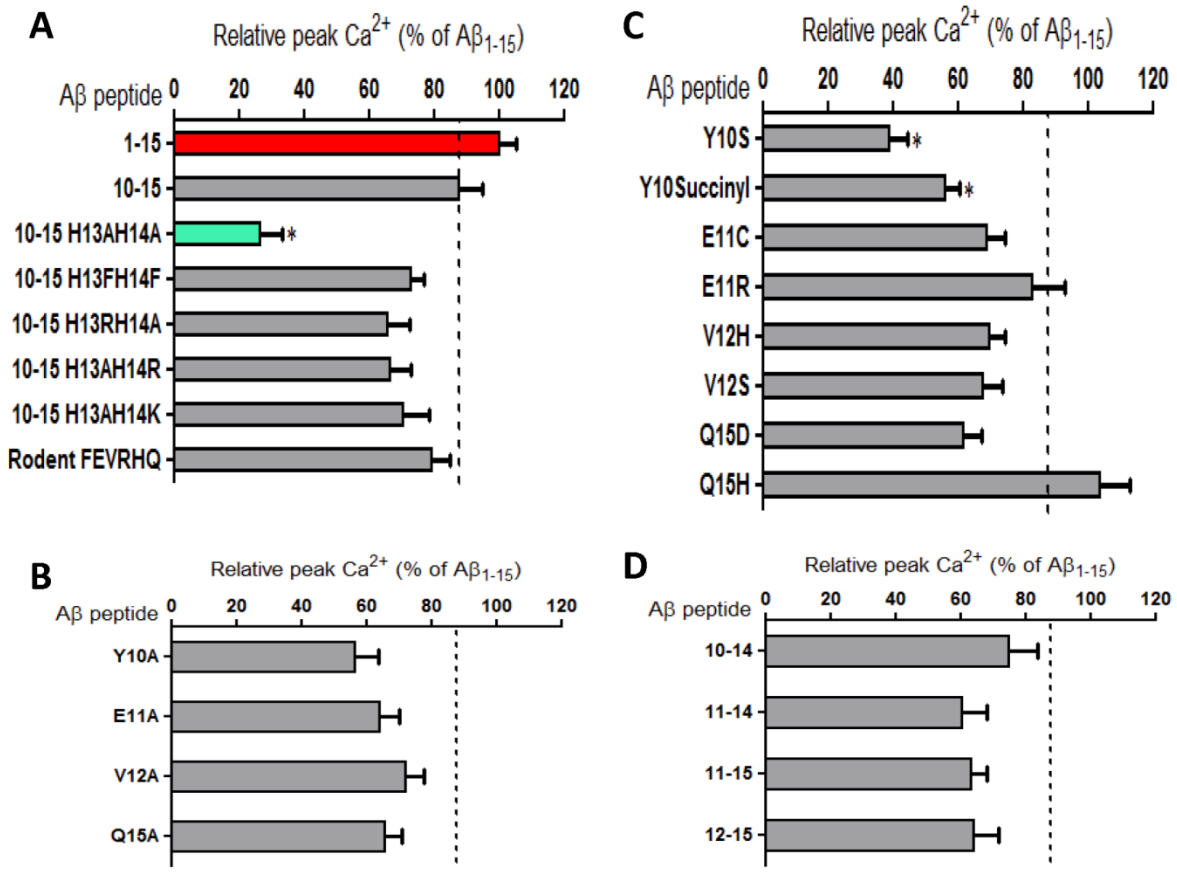

Figure 20. Average peak Ca^{2+} responses in varicosities of NG108-15 cells expressing α7-nAChR to $A\beta_{10-15}$ mutants and truncations

Average peak Ca^{2+} responses in varicosities of NG108-15 cells expressing α7-nAChR to 100nM: **(A)** $A\beta_{1-15}$ (n = 178), $A\beta_{10-15}$ (n = 70),$A\beta_{10-15}$ H13AH14A (n = 19), $A\beta_{10-15}$ H13FH14F (n = 38), $A\beta_{10-15}$ H13RH14A (n = 11), $A\beta_{10-15}$ H13AH14R (n = 22), $A\beta_{10-15}$ H13AH14K (n = 22), $A\beta_{10-15}$ FEVRHQ (n = 26); **(B)** $A\beta_{10-15}$ Y10A (n = 14), $A\beta_{10-15}$ E11A (n = 25), $A\beta_{10-15}$ V12A (n = 21), $A\beta_{10-15}$ Q15A (n = 36); **(C)** $A\beta_{10-15}$ Y10S (n = 10), $A\beta_{10-15}$ Y10Succinyl (n = 24), $A\beta_{10-15}$ E11c (n = 20), $A\beta_{10-15}$ E11R (n = 11), $A\beta_{10-15}$ V12H (n = 10), $A\beta_{10-15}$ V12S (n = 24), $A\beta_{10-15}$ Q15D (n = 24), $A\beta_{10-15}$ Q1H (n = 33); **(D)** $A\beta_{10-14}$ (n = 19), $A\beta_{11-14}$ (n = 11), $A\beta_{11-15}$ (n = 20), $A\beta_{12-15}$ (n = 18). $^{*}p < 0.05$ (Bonferoni *post hoc* tests) NB. Dashed lines indicate the baseline (background) and average maximal responses for $A\beta_{10-15}$.

4. Discussion

The finding that both $A\beta_{1-15}$ and $A\beta_{12-28}$ display agonist-like activity led to the possibility that a tiny fragment of Aβ may also retain such activity. As neprilysin can cleave between positions 9 and 10 on Aβ[24], it was logical to start by examining the activity of the $A\beta_{10-15}$ fragment. The presence of a robust activity with this fragment both *in vitro* and *in vivo* in turn led us to examine the effects of each amino acid within this sequence.

The trend for a reduction in the response of $A\beta_{10-15}$ compared to $A\beta_{1-15}$, coupled with the data in Fig. 10 for the trend to a reduction in activity with the H6A mutant, could indicate a role for His-6 in the activation of α7nAChR. It is also possible that the two phenylalanines (Phe-19 & Ph-20) may play a similar role in the activity of the $A\beta_{12-28}$ fragment. This role may be interacting with the other aromatic residues previously discovered to be located within the receptor's binding pocket[54] to orient the two histidines at positions 13 and 14. This explanation would likewise be relevant to Tyr-10, whose mutation to serine or a succinyl group significantly reduced activity; however, the loss of this tyrosine did not produce a significant reduction in activity in our model, although there was a trend in that direction. The truncation of the tyrosine may of course lead to a change in shape of the peptide that in turn reduces the necessity of the residue to properly align the fragment within the binding pocket.

The other finding of note was the trend toward an enhanced response to the Q15H substitution, compared to the trend toward a reduced response with the V12H substitution. The implication is that adding an extra histidine at the C-terminal of the other two histidine residues, as opposed to the N-terminal side may increase the activation of the key tyrosine within the α7nAChR binding pocket.

A BLAST search on Uniprot protein and peptide database [109] for the $A\beta_{10-15}$ sequence revealed 429 matches. Of these there were some uncharacterized proteins from across many species and phyla, whilst of the characterized proteins the vast majority of matches were from APP or Aβ proteins across many species, with a few proteins from potato or plant mottle viruses and single entries for a subunit of tetrathionate reductase, ATPase AAA domain, N-acetylneuraminate synthase and the mucus secretion of the common vampire bat. Such a small number of matches on a hexamer is quite remarkable, leading to the possibility of a high level of specificity of action for this fragment.

Equally as intriguing is the finding by Shin and Saxena that His-6, His-13 and His-14 are supposed contributors to a putative Cu and perhaps Zn binding site in $A\beta_{1-42}$[110] leading to the potential involvement of these metals in the interaction of Aβ and its fragments with nAChRs. In addition, the $A\beta_{10-15}$ sequence of YEVHHQ overlaps with a putative heparin-binding consensus sequence VHHQKL[111], the significance of which remains unclear.

Chapter 4

Conclusions

1. Concluding Remarks

Our work has demonstrated that the N-terminal domain of Abeta accounts for the peptide's agonist-like activity toward nAChRs. Moreover, the N-terminal 1-15 fragment, found in CSF, was shown itself to be a potent actiator of nAChRs more effective than full-length $A\beta_{1-42}$. Lastly, our work has shown that there are two residues, His-13 and His-14, that are essential for the agonist-like activity of Aβ upon nAChR and that this activity is more potent in the N-terminal fragments, which are produced as a result of the concomitant activity of α- and β-secretases[37].

We have also demonstrated that the activity of the N-terminal fragments may have physiological consequences as it augmented both theta burst-induced post-tetanic potentiation and LTP in mouse hippocampal slices and also rescued LTP inhibited by elevated levels of full-length Aβ. In addition, bilateral injection of the N-terminal fragment into the dorsal hippocampi of intact mice enhanced contextual fear conditioning, which itself was attenuated by coadministration of a nicotinic antagonist.

These findings indicate that the N-terminal Aβ fragments may act as potent and effective endogenous neuromodulators most likely acting via activation of presynaptic nAChRs. Accordingly, increasing the activity of α-secretase over γ-secretase, possibly through γ-secretase inhibition may lead to the realization of an effective therapeutic strategy for the treatment of AD. It may even be possible to directly apply these fragments or peptidomimetics derived therefrom to counter the neurotoxic effects of the accumulation of Aβ found in AD.

2. Future Directions

Many avenues for further investigation have been highlighted by our work. We intend to examine the potency of the mutated $A\beta_{10-15}$ fragments by examining the agonist-like activity of varying concentrations of them on our α7-nAChR transfected NG108 presynaptic model.

We would also like to develop a selection of peptidomimetics as analogues of these fragments and determine their effects *in vitro* and *in vivo*.

An examination of interactions between the N-terminal fragments and the α7-nAChR, is also required. To this end we have established a collaboration with Dr Lin Chen, Professor of Biological Sciences and Chemistry, and Dr Shuxing Li, NanoBiophysics Core, USC, who will attempt to co-crystallize the fragments with the α7-AChBP chimera they have developed[57] and then examine the resultant crystals by X-ray crystallography.

We had hoped to examine the binding affinities of the N-terminal fragments and full length Aβ with α7-nAChRs via competitive radio-ligand binding assays with our collaborator Dr. Daniela Guendisch, Assistant Professor of Pharmaceutical Sciences at UH Hilo. We were, however, unsuccessful possibly due to one, or a combination of, issues including low binding affinities of our peptides compared to the tritiated epibatidine (an nAChR agonist with an extremely high affinity for α4β2 receptors), poor quality tritiated epibatidine or insufficient starting material from rodent hippocampi. We have proposals to increase the amount of starting material by using pig hippocampi and examine binding affinities directly using tritiated Aβ fragments.

We have also attempted to search for the presence of the fragments in mouse brain via immunoprecipitation followed by MALDI-TOF, but were unsuccessful to-date, which may be due to insufficient starting material or the extremely low levels of these fragments in the brain.

Further investigation of the effects of altering the activity of endogenous α- and β-secretases on the production of these fragments is also required, as is the effect of any upregulation on both signaling and cell survival. Indeed, the potential of these fragments to act as a neuroprotectants is currently being examined in our lab using the model established in Arora et al[108].

In addition, it will be illuminating, given the detrimental effect of familial mutations on the increased production of the toxic $A\beta_{1-42}$, whether these mutations (e.g. A21G Flemish mutation, E22K Italian mutation, E22Q Dutch mutation and E22G Arctic mutation) also effect the production of the N-terminal fragments.

The intriguing possibility of the involvement of Cu or Zn binding being involved in activation of nAChR by Aβ should be investigated, potentially through the combined use of chelators and the mutant Aβ fragments.

Finally, the effects of the N-terminal fragments on other known receptor targets, especially NMDAR, mGluR and amylin receptors as well as cellular prion protein (which has been found to activate Fyn to impair neurons[112]) need to be assessed.

Publications to date

James L.M. Lawrence,[1] Mei Tong,[1] Naghum Alfulaij, Tessi Sherrin, Mark Contarino, Michael M. White, Frederick P. Bellinger, Cedomir Todorovic, and Robert A. Nichols. Regulation of Presynaptic Ca^{2+}, Synaptic Plasticity and Contextual Fear Conditioning by a N-terminal β-Amyloid Fragment. J. Neuroscience October 22 2014 34 (43): 14210-14218: ([1]co-first authors) [Featured Article]

References

1. 2012 Alzheimer's disease facts and figures. *Alzheimer's & Dementia* **8,** 131–168 (2012).
2. Alzheimer, A., Stelzmann, R. A., Schnitzlein, H. N. & Murtagh, F. R. An English translation of Alzheimer's 1907 paper, 'Uber eine eigenartige Erkankung der Hirnrinde'. *Clin Anat* **8,** 429–431 (1995).
3. Jack, C. R., Jr *et al.* Introduction to the recommendations from the National Institute on Aging-Alzheimer's Association workgroups on diagnostic guidelines for Alzheimer's disease. *Alzheimers Dement* **7,** 257–262 (2011).
4. Albert, M. S. *et al.* The diagnosis of mild cognitive impairment due to Alzheimer's disease: recommendations from the National Institute on Aging-Alzheimer's Association workgroups on diagnostic guidelines for Alzheimer's disease. *Alzheimers Dement* **7,** 270–279 (2011).
5. McKhann, G. M. *et al.* The diagnosis of dementia due to Alzheimer's disease: recommendations from the National Institute on Aging-Alzheimer's Association workgroups on diagnostic guidelines for Alzheimer's disease. *Alzheimers Dement* **7,** 263–269 (2011).
6. Holtzman, D. M., Morris, J. C. & Goate, A. M. Alzheimer's disease: the challenge of the second century. *Science Translational Medicine* **3,** 77sr1 (2011).
7. Price, J. L. *et al.* Neuron number in the entorhinal cortex and CA1 in preclinical Alzheimer disease. *Arch. Neurol.* **58,** 1395–1402 (2001).
8. Coyle, J. T., Price, D. L. & DeLong, M. R. Alzheimer's disease: a disorder of cortical cholinergic innervation. *Science* **219,** 1184–1190 (1983).
9. Buckner, R. L. *et al.* Molecular, structural, and functional characterization of Alzheimer's disease: evidence for a relationship between default activity, amyloid, and memory. *J. Neurosci.* **25,** 7709–7717 (2005).
10. Raichle, M. E. *et al.* A default mode of brain function. *Proc. Natl. Acad. Sci. U.S.A.* **98,** 676–682 (2001).
11. Sperling, R. A. *et al.* Amyloid deposition is associated with impaired default network function in older persons without dementia. *Neuron* **63,** 178–188 (2009).
12. Bero, A. W. *et al.* Neuronal activity regulates the regional vulnerability to amyloid-β deposition. *Nat. Neurosci.* **14,** 750–756 (2011).
13. Perrin, R. J., Fagan, A. M. & Holtzman, D. M. Multimodal techniques for diagnosis and prognosis of Alzheimer's disease. *Nature* **461,** 916–922 (2009).

14. Walsh, D. M. & Selkoe, D. J. A beta oligomers - a decade of discovery. *J. Neurochem.* **101,** 1172–1184 (2007).
15. Mawuenyega, K. G. *et al.* Decreased Clearance of CNS β-Amyloid in Alzheimer's Disease. *Science* **330,** 1774–1774 (2010).
16. Roses, A. D. & Saunders, A. M. APOE is a major susceptibility gene for Alzheimer's disease. *Curr. Opin. Biotechnol.* **5,** 663–667 (1994).
17. Cramer, P. E. *et al.* ApoE-Directed Therapeutics Rapidly Clear β-Amyloid and Reverse Deficits in AD Mouse Models. *Science Signalling* **335,** 1503 (2012).
18. Kim, J., Basak, J. M. & Holtzman, D. M. The role of apolipoprotein E in Alzheimer's disease. *Neuron* **63,** 287–303 (2009).
19. Haass, C. *et al.* Amyloid beta-peptide is produced by cultured cells during normal metabolism. *Nature* **359,** 322–325 (1992).
20. Bjerke, M. *et al.* Confounding factors influencing amyloid Beta concentration in cerebrospinal fluid. *Int J Alzheimers Dis* **2010,** (2010).
21. Puzzo, D. *et al.* Picomolar amyloid-beta positively modulates synaptic plasticity and memory in hippocampus. *J. Neurosci.* **28,** 14537–14545 (2008).
22. Schubert, W. *et al.* Localization of Alzheimer beta A4 amyloid precursor protein at central and peripheral synaptic sites. *Brain Res.* **563,** 184–194 (1991).
23. Neve, R. L., Finch, E. A. & Dawes, L. R. Expression of the Alzheimer amyloid precursor gene transcripts in the human brain. *Neuron* **1,** 669–677 (1988).
24. De Strooper, B. & Annaert, W. Proteolytic processing and cell biological functions of the amyloid precursor protein. *J. Cell. Sci.* **113 (Pt 11),** 1857–1870 (2000).
25. Portelius, E., Westman-Brinkmalm, A., Zetterberg, H. & Blennow, K. Determination of beta-amyloid peptide signatures in cerebrospinal fluid using immunoprecipitation-mass spectrometry. *J. Proteome Res.* **5,** 1010–1016 (2006).
26. Allinson, T. M. J., Parkin, E. T., Turner, A. J. & Hooper, N. M. ADAMs family members as amyloid precursor protein alpha-secretases. *J. Neurosci. Res.* **74,** 342–352 (2003).
27. Schlöndorff, J. & Blobel, C. P. Metalloprotease-disintegrins: modular proteins capable of promoting cell-cell interactions and triggering signals by protein-ectodomain shedding. *J. Cell. Sci.* **112 (Pt 21),** 3603–3617 (1999).
28. Sisodia, S. S. Beta-amyloid precursor protein cleavage by a membrane-bound protease. *Proc. Natl. Acad. Sci. U.S.A.* **89,** 6075–6079 (1992).
29. Skovronsky, D. M., Moore, D. B., Milla, M. E., Doms, R. W. & Lee, V. M.-Y. Protein Kinase C-dependent α-Secretase Competes with β-Secretase for Cleavage of Amyloid-β Precursor Protein in the Trans-Golgi Network. *J. Biol. Chem.* **275,** 2568–2575 (2000).
30. Vassar, R. *et al.* Beta-secretase cleavage of Alzheimer's amyloid precursor protein by the transmembrane aspartic protease BACE. *Science* **286,** 735–741 (1999).
31. Cole, S. L. & Vassar, R. The Alzheimer's disease β-secretase enzyme, BACE1. *Molecular neurodegeneration* **2,** 22 (2007).
32. Ehehalt, R., Keller, P., Haass, C., Thiele, C. & Simons, K. Amyloidogenic processing of the Alzheimer β-amyloid precursor protein depends on lipid rafts. *J Cell Biol* **160,** 113–123 (2003).
33. Mullan, M. *et al.* A pathogenic mutation for probable Alzheimer's disease in the APP gene at the N-terminus of beta-amyloid. *Nat. Genet.* **1,** 345–347 (1992).
34. Vetrivel, K. S. *et al.* Association of γ-Secretase with Lipid Rafts in Post-Golgi and Endosome Membranes. *J. Biol. Chem.* **279,** 44945–44954 (2004).
35. Wolfe, M. S. *et al.* Two transmembrane aspartates in presenilin-1 required for presenilin endoproteolysis and gamma-secretase activity. *Nature* **398,** 513–517 (1999).

36. Hartmann, T. *et al.* Distinct sites of intracellular production for Alzheimer's disease A beta40/42 amyloid peptides. *Nat. Med.* **3,** 1016–1020 (1997).
37. Portelius, E. *et al.* A novel pathway for amyloid precursor protein processing. *Neurobiology of Aging* **32,** 1090–1098 (2011).
38. Portelius, E. *et al.* Amyloid-β(1-15/16) as a marker for γ-secretase inhibition in Alzheimer's disease. *J. Alzheimers Dis.* **31,** 335–341 (2012).
39. Woronowicz, A. *et al.* Absence of carboxypeptidase E leads to adult hippocampal neuronal degeneration and memory deficits. *Hippocampus* **18,** 1051–1063 (2008).
40. Papp, H. *et al.* Expression and distribution of carboxypeptidase B in the hippocampal subregions of normal and Alzheimer's disease brain. *Acta. Biol. Hung.* **54,** 55–62 (2003).
41. Cirrito, J. R. *et al.* Synaptic activity regulates interstitial fluid amyloid-beta levels in vivo. *Neuron* **48,** 913–922 (2005).
42. Cirrito, J. R. *et al.* Endocytosis is required for synaptic activity-dependent release of amyloid-beta in vivo. *Neuron* **58,** 42–51 (2008).
43. Hsieh, H. *et al.* AMPAR removal underlies Abeta-induced synaptic depression and dendritic spine loss. *Neuron* **52,** 831–843 (2006).
44. Shankar, G. M. *et al.* Natural oligomers of the Alzheimer amyloid-beta protein induce reversible synapse loss by modulating an NMDA-type glutamate receptor-dependent signaling pathway. *J. Neurosci.* **27,** 2866–2875 (2007).
45. Kamenetz, F. *et al.* APP processing and synaptic function. *Neuron* **37,** 925–937 (2003).
46. Puzzo, D. *et al.* Endogenous amyloid-β is necessary for hippocampal synaptic plasticity and memory. *Annals of neurology* **69,** 819–830 (2011).
47. Palop, J. J. & Mucke, L. Amyloid-beta-induced neuronal dysfunction in Alzheimer's disease: from synapses toward neural networks. *Nat. Neurosci.* **13,** 812–818 (2010).
48. Chin, J. H., Ma, L., MacTavish, D. & Jhamandas, J. H. Amyloid beta protein modulates glutamate-mediated neurotransmission in the rat basal forebrain: involvement of presynaptic neuronal nicotinic acetylcholine and metabotropic glutamate receptors. *J. Neurosci.* **27,** 9262–9269 (2007).
49. Kimura, R., Mactavish, D., Yang, J., Westaway, D. & Jhamandas, J. H. Beta Amyloid-Induced Depression of Hippocampal Long-Term Potentiation Is Mediated through the Amylin Receptor. *J. Neurosci.* **32,** 17401–17406 (2012).
50. Gotti, C. & Clementi, F. Neuronal nicotinic receptors: from structure to pathology. *Progress in Neurobiology* **74,** 363–396 (2004).
51. Unwin, N. Acetylcholine receptor channel imaged in the open state. *Nature* **373,** 37–43 (1995).
52. *Fundamental neuroscience*. (Elsevier, 2012).
53. Unwin, N. Refined structure of the nicotinic acetylcholine receptor at 4A resolution. *J. Mol. Biol.* **346,** 967–989 (2005).
54. Taly, A., Corringer, P.-J., Guedin, D., Lestage, P. & Changeux, J.-P. Nicotinic receptors: allosteric transitions and therapeutic targets in the nervous system. *Nat Rev Drug Discov* **8,** 733–750 (2009).
55. Brejc, K. *et al.* Crystal structure of an ACh-binding protein reveals the ligand-binding domain of nicotinic receptors. *Nature* **411,** 269–276 (2001).
56. Tong, M., Arora, K., White, M. M. & Nichols, R. A. Role of key aromatic residues in the ligand-Binding domain of 7 nicotinic receptors in the agonist action of -aAmyloid. *Journal of Biological Chemistry* (2011). doi:10.1074/jbc.M111.241299
57. Li, S.-X. *et al.* Ligand-binding domain of an α7-nicotinic receptor chimera and its complex with agonist. *Nature Neuroscience* **14,** 1253–1259 (2011).
58. Valor, L. M. *et al.* Role of the large cytoplasmic loop of the alpha 7 neuronal nicotinic acetylcholine receptor subunit in receptor expression and function. *Biochemistry* **41,** 7931–7938 (2002).

59. Wecker, L., Guo, X., Rycerz, A. M. & Edwards, S. C. Cyclic AMP-dependent protein kinase (PKA) and protein kinase C phosphorylate sites in the amino acid sequence corresponding to the M3/M4 cytoplasmic domain of alpha4 neuronal nicotinic receptor subunits. *J. Neurochem.* **76,** 711–720 (2001).
60. Barik, J. & Wonnacott, S. Molecular and cellular mechanisms of action of nicotine in the CNS. *Handb Exp Pharmacol* 173–207 (2009).
61. Quick, M. W. & Lester, R. A. J. Desensitization of neuronal nicotinic receptors. *J. Neurobiol.* **53,** 457–478 (2002).
62. Fucile, S., Renzi, M., Lax, P. & Eusebi, F. Fractional Ca(2+) current through human neuronal alpha7 nicotinic acetylcholine receptors. *Cell Calcium* **34,** 205–209 (2003).
63. Giniatullin, R., Nistri, A. & Yakel, J. L. Desensitization of nicotinic ACh receptors: shaping cholinergic signaling. *Trends Neurosci.* **28,** 371–378 (2005).
64. Bouzat, C., Bartos, M., Corradi, J. & Sine, S. M. The interface between extracellular and transmembrane domains of homomeric Cys-loop receptors governs open-channel lifetime and rate of desensitization. *J. Neurosci.* **28,** 7808–7819 (2008).
65. Fabian-Fine, R. *et al.* Ultrastructural distribution of the alpha7 nicotinic acetylcholine receptor subunit in rat hippocampus. *J. Neurosci.* **21,** 7993–8003 (2001).
66. Wang, H. Y., Lee, D. H., Davis, C. B. & Shank, R. P. Amyloid peptide Abeta(1-42) binds selectively and with picomolar affinity to alpha7 nicotinic acetylcholine receptors. *J. Neurochem.* **75,** 1155–1161 (2000).
67. Khan, G. M., Tong, M., Jhun, M., Arora, K. & Nichols, R. A. beta-Amyloid activates presynaptic alpha7 nicotinic acetylcholine receptors reconstituted into a model nerve cell system: involvement of lipid rafts. *Eur. J. Neurosci* **31,** 788–796 (2010).
68. Religa, D. *et al.* Amyloid beta pathology in Alzheimer's disease and schizophrenia. *Am J Psychiatry* **160,** 867–872 (2003).
69. Dellisanti, C. D., Yao, Y., Stroud, J. C., Wang, Z.-Z. & Chen, L. Crystal structure of the extracellular domain of nAChR alpha1 bound to alpha-bungarotoxin at 1.94 A resolution. *Nat. Neurosci.* **10,** 953–962 (2007).
70. Celie, P. H. N. *et al.* Nicotine and carbamylcholine binding to nicotinic acetylcholine receptors as studied in AChBP crystal structures. *Neuron* **41,** 907–914 (2004).
71. Morimoto, A. *et al.* Analysis of the secondary structure of beta-amyloid (Abeta42) fibrils by systematic proline replacement. *J. Biol. Chem.* **279,** 52781–52788 (2004).
72. Murakami, K., Masuda, Y., Shirasawa, T., Shimizu, T. & Irie, K. The turn formation at positions 22 and 23 in the 42-mer amyloid beta peptide: the emerging role in the pathogenesis of Alzheimer's disease. *Geriatr Gerontol Int* **10 Suppl 1,** S169–179 (2010).
73. Nelson, P., Christian, C. & Nirenberg, M. Synapse formation between clonal neuroblastoma X glioma hybrid cells and striated muscle cells. *Proc. Natl. Acad. Sci. U.S.A.* **73,** 123–127 (1976).
74. McGee, R. *et al.* Regulation of acetylcholine release from neuroblastoma x glioma hybrid cells. *Proc. Natl. Acad. Sci. U.S.A.* **75,** 1314–1318 (1978).
75. Ronde, P., Dougherty, J. J. & Nichols, R. A. Functional IP3- and ryanodine-sensitive calcium stores in presynaptic varicosities of NG108-15 (rodent neuroblastoma x glioma hybrid) cells. *The Journal of Physiology* **529,** 307–319 (2000).
76. Rondé, P. & Nichols, R. A. Postsynaptic target regulates functional responses induced by 5-HT3 serotonin receptors on axonal varicosities of NG108-15 hybrid neuroblastoma cells. *Neuroscience* **102,** 979–987 (2001).
77. Selkoe, D. J. Alzheimer's disease is a synaptic failure. *Science* **298,** 789–791 (2002).
78. Selkoe, D. J. Soluble oligomers of the amyloid β-protein impair synaptic plasticity and behavior. *Behavioural brain research* **192,** 106–113 (2008).

79. Bateman, R. J. *et al.* Human amyloid-beta synthesis and clearance rates as measured in cerebrospinal fluid in vivo. *Nat. Med.* **12,** 856–861 (2006).
80. Lazarov, O., Lee, M., Peterson, D. A. & Sisodia, S. S. Evidence that synaptically released beta-amyloid accumulates as extracellular deposits in the hippocampus of transgenic mice. *J. Neurosci.* **22,** 9785–9793 (2002).
81. Golde, T. E., Eckman, C. B. & Younkin, S. G. Biochemical detection of Aβ isoforms: implications for pathogenesis, diagnosis, and treatment of Alzheimer's disease. *Biochimica et Biophysica Acta (BBA) - Molecular Basis of Disease* **1502,** 172–187 (2000).
82. Koo, E. H. *et al.* Precursor of amyloid protein in Alzheimer disease undergoes fast anterograde axonal transport. *PNAS* **87,** 1561–1565 (1990).
83. Selkoe, D. J. & Schenk, D. Alzheimer's disease: molecular understanding predicts amyloid-based therapeutics. *Annu. Rev. Pharmacol. Toxicol.* **43,** 545–584 (2003).
84. Selkoe, D. J. Alzheimer's disease: genes, proteins, and therapy. *Physiol. Rev.* **81,** 741–766 (2001).
85. Thinakaran, G. & Koo, E. H. Amyloid precursor protein trafficking, processing, and function. *J. Biol. Chem.* **283,** 29615–29619 (2008).
86. Portelius, E. *et al.* Distinct cerebrospinal fluid amyloid beta peptide signatures in sporadic and PSEN1 A431E-associated familial Alzheimer's disease. *Mol Neurodegener* **5,** 2 (2010).
87. Portelius, E. *et al.* Characterization of amyloid beta peptides in cerebrospinal fluid by an automated immunoprecipitation procedure followed by mass spectrometry. *J. Proteome Res.* **6,** 4433–4439 (2007).
88. Portelius, E. *et al.* A novel Abeta isoform pattern in CSF reflects gamma-secretase inhibition in Alzheimer disease. *Alzheimers Res Ther* **2,** 7 (2010).
89. Patel, A. N. & Jhamandas, J. H. Neuronal receptors as targets for the action of amyloid-beta protein (Aβ) in the brain. *Expert Rev Mol Med* **14,** e2 (2012).
90. Liu, Q., Kawai, H. & Berg, D. K. β-Amyloid peptide blocks the response of α7-containing nicotinic receptors on hippocampal neurons. *Proceedings of the National Academy of Sciences* **98,** 4734–4739 (2001).
91. Pettit, D. L., Shao, Z. & Yakel, J. L. beta-Amyloid(1-42) peptide directly modulates nicotinic receptors in the rat hippocampal slice. *J. Neurosci.* **21,** RC120 (2001).
92. Dougherty, J. J., Wu, J. & Nichols, R. A. β-Amyloid Regulation of Presynaptic Nicotinic Receptors in Rat Hippocampus and Neocortex. *J. Neurosci.* **23,** 6740–6747 (2003).
93. Mehta, T. K. *et al.* Defining pre-synaptic nicotinic receptors regulated by beta amyloid in mouse cortex and hippocampus with receptor null mutants. *J. Neurochem.* **109,** 1452–1458 (2009).
94. Tsumoto, K. *et al.* Role of arginine in protein refolding, solubilization, and purification. *Biotechnol. Prog.* **20,** 1301–1308 (2004).
95. Dunkley, P. R., Jarvie, P. E. & Robinson, P. J. A rapid Percoll gradient procedure for preparation of synaptosomes. *Nat Protoc* **3,** 1718–1728 (2008).
96. Rowan, M. J., Klyubin, I., Wang, Q., Hu, N. W. & Anwyl, R. Synaptic memory mechanisms: Alzheimer's disease amyloid beta-peptide-induced dysfunction. *Biochem. Soc. Trans.* **35,** 1219–1223 (2007).
97. Sherrin, T. *et al.* Hippocampal c-Jun-N-terminal kinases serve as negative regulators of associative learning. *J. Neurosci.* **30,** 13348–13361 (2010).
98. Ma, T. *et al.* Dysregulation of the mTOR pathway mediates impairment of synaptic plasticity in a mouse model of Alzheimer's disease. *PLoS ONE* **5,** (2010).
99. Puzzo, D. *et al.* Endogenous amyloid-β is necessary for hippocampal synaptic plasticity and memory. *Ann. Neurol.* **69,** 819–830 (2011).

100. Abramov, E. *et al.* Amyloid-beta as a positive endogenous regulator of release probability at hippocampal synapses. *Nat. Neurosci.* **12,** 1567–1576 (2009).
101. Pirttimaki, T. M. *et al.* α7 Nicotinic receptor-mediated astrocytic gliotransmitter release: Aβ effects in a preclinical Alzheimer's mouse model. *PLoS ONE* **8,** e81828 (2013).
102. Lawrence, J. L. M. *et al.* Regulation of Presynaptic Ca2+, Synaptic Plasticity and Contextual Fear Conditioning by a N-terminal β-Amyloid Fragment. *J. Neurosci.* **34,** 14210–14218 (2014).
103. Marcinkiewicz, M. & Seidah, N. G. Coordinated expression of beta-amyloid precursor protein and the putative beta-secretase BACE and alpha-secretase ADAM10 in mouse and human brain. *J. Neurochem.* **75,** 2133–2143 (2000).
104. Tippmann, F., Hundt, J., Schneider, A., Endres, K. & Fahrenholz, F. Up-regulation of the alpha-secretase ADAM10 by retinoic acid receptors and acitretin. *FASEB J.* **23,** 1643–1654 (2009).
105. Wang, Q. *et al.* Alpha v integrins mediate beta-amyloid induced inhibition of long-term potentiation. *Neurobiol. Aging* **29,** 1485–1493 (2008).
106. Whitson, J. S., Selkoe, D. J. & Cotman, C. W. Amyloid beta protein enhances the survival of hippocampal neurons in vitro. *Science* **243,** 1488–1490 (1989).
107. Harmeier, A. *et al.* Role of amyloid-beta glycine 33 in oligomerization, toxicity, and neuronal plasticity. *J. Neurosci.* **29,** 7582–7590 (2009).
108. Arora, K., Alfulaij, N., Higa, J. K., Panee, J. & Nichols, R. A. Impact of sustained exposure to β-amyloid on calcium homeostasis and neuronal integrity in model nerve cell system expressing α4β2 nicotinic acetylcholine receptors. *J. Biol. Chem.* **288,** 11175–11190 (2013).
109. blastp results [completed]. at <http://www.uniprot.org/blast/uniprot/B201411102E3QMDNFF0>
110. Shin, B. & Saxena, S. Substantial contribution of the two imidazole rings of the His13-His14 dyad to Cu(II) binding in amyloid-β(1-16) at physiological pH and its significance. *J Phys Chem A* **115,** 9590–9602 (2011).
111. Buée, L., Ding, W., Delacourte, A. & Fillit, H. Binding of secreted human neuroblastoma proteoglycans to the Alzheimer's amyloid A4 peptide. *Brain Res.* **601,** 154–163 (1993).
112. Um, J. W. *et al.* Alzheimer amyloid-β oligomer bound to postsynaptic prion protein activates Fyn to impair neurons. *Nat. Neurosci.* **15,** 1227–1235 (2012).